Universitat Rovira i Virgili
Departament d'Història i Història de l'Art
Màster en Arqueologia del Quaternari i Evolució Humana (Erasmus Mundus)

International Master in
QUATERNARY AND PREHISTORY

Tesis de Master:

MORE THAN ONE SPECIES? VARIATION IN DMANISI CRANIA ANALYSED BY RANDOMIZATION METHODS

Julian Melbourne Skelton

Director: Carlos Lorenzo Merino

Curso académico 2021/2022

ACKNOWLEDGEMENT

This document lies before your eyes thanks to a journey that I started at age 9 when my mother gave me for Christmas a book entitled “Les Hommes Préhistoriques” by Josef Augusta, published in 1966 by Éditions La Farandole, Paris. The illustrations and text provoked an interest that has lasted until this day.

However, for different reasons, that interest in prehistory lay dormant for many years, awakening from time to time during visits to museums and bookshops, or following reports of the latest archaeological discoveries on radio and television.

Half a century after receiving the above book for Christmas, a plethora of circumstances led me to an interview with Carlos Lorenzo, who confirmed my academic suitability to join the International Master in Quaternary and Prehistory. He warmly encouraged me to consider returning to university after an absence of 33 years. I am indebted to Carlos for his advice, and also for his energy, input and time as advisor for this thesis.

In my pre-IMQP life I have worked in four European countries in different sectors for American, British, French and Italian multinationals. Coordinating teams from different countries and organizational cultures is always challenging and I congratulate the IMQP organization and consortium members for an outstanding Master programme. I witnessed excellent consortium teamwork in handling the impact of the Covid pandemic on the study schedule and also during my Erasmus period at Muséum National d’Histoire Naturelle.

Finally, I would like to thank the staff, professors and my fellow students in Tarragona and Paris for their time and patience in handling my questions, doubts and comments. Your contribution to my learning experience was invaluable.

MORE THAN ONE SPECIES? VARIATION IN DMANISI CRANIA ANALYSED BY RANDOMIZATION METHODS

ABSTRACT

The early Pleistocene site of Dmanisi has yielded five hominin skulls deposited in close proximity within a short chronology. The morphological and size variation displayed by these five skulls fuel a continuing debate as to the number of taxa represented. The null hypothesis of this study is that just one species is present and randomization methods are used to compare the variability of ten fossil cranial measurements to those of five modern human reference populations, selected on the basis of ecology or extreme size. Though the archaeological record of Africa and Eurasia suggests that it is reasonable to pre-suppose the presence of more than one taxon at a site such as Dmanisi, and despite different patterns of variability displayed by the Dmanisi and modern human crania, the null hypothesis cannot be rejected: the Dmanisi hominins represent a single species.

KEYWORDS

Dmanisi; variation; bootstrap; cranial measurement; variability

CONTENTS

1 INTRODUCTION

1.1 The study of metric variation in fossils

The sorting of fossil specimens according to qualitative and quantitative criteria is an important step in their classification into species. Metric variation in a collection of fossil specimens can be used for species recognition when their relative variation is compared to that of an extant species. In making such a comparison, we are testing whether the fossil metric variation is so great that it cannot be contained within a single species (Plavcan & Cope, 2001).

The task of identifying hominin species in the archaeological record is problematic due to the scarcity of remains spread over large geographic areas and their often fragmented condition as a result of the effects of taphonomy. However, in the case of Dmanisi, despite yielding five hominin skulls in close proximity within a narrow stratigraphy, there is a continuing debate concerning the number of species present in the assemblage as we shall see below in section 1.4

1.2 Objectives of this thesis

This study aims to contribute to the aforementioned debate and will explore the variability of the 5 Dmanisi crania to establish whether one or more species might be present. Published cranial measurements of the Dmanisi skulls will be compared to those of different reference groups of modern human populations. The randomization method of bootstrapping will be used to allow meaningful comparison between the small Dmanisi fossil sample and the far larger modern reference groups.

The null hypothesis will be that the five Dmanisi skulls represent a single species. To reject this hypothesis will require showing that variability in the cranial measurements at Dmanisi is higher than that of the selected modern human groups.

1.3 Dmanisi context

Dmanisi is an Early Pleistocene site in the Georgian Caucasus that has yielded human fossils together with stone artefacts and a diversity of faunal remains. Dated to approximately 1,8 million years ago, it represents the earliest occurrence of the genus *Homo* outside of Africa.

Investigations into the sedimentary context together with paleomagnetic and radiometric studies have concluded that the hominin remains, all found in close proximity to each other, could have been rapidly deposited in a time frame of between 10,000 to 80,000 years. These two robust constraints of proximity and time are commonly mentioned in morphological and anatomical studies of the Dmanisi fossils as additional support of the hypothesis of a single species at Dmanisi.

1.4 Debate concerning range of variation in Dmanisi hominins

However, despite the aforementioned spatial and temporal constraints, the considerable range of metric and morphological variation present in the Dmanisi teeth, mandibles and crania has provoked an intense debate concerning the number of hominin taxa present at the site. Acknowledging this debate, one of the scientists involved with the research published for skull 5 even remarked that had

the remains been found in separate African locations, they could have been defined as separate species (Gibbons, 2013).

A study of dental dimensions and root morphology (Martinón-Torres et al., 2008) suggested the existence of two distinct paleodemes at Dmanisi. Research performed on the mandibles has confirmed they show substantially more size variation when compared to modern humans and that general mandible size in addition to corpus shape and height variability are significantly greater than those of any species of extant ape (Skinner et al., 2006). A further study of the mandibles, examining the impact of ontogeny on their morphology, revealed significant shape differences, unrelated to size or sexual dimorphism, between mandible D2600 and mandibles D211 and D2735 (Figure 3). The authors concluded that their work provided additional support to the hypothesis of more than one paleodeme at Dmanisi (Bermúdez De Castro et al., 2014).

The variability in the shape of the cranial vault and the supraorbital morphology also point to a diversity of taxa, especially in the case of skull 5 (Schwartz et al., 2014). The authors of the study even go so far as stating that not attributing a separate identity to this hominin implies effectively denying the utility of morphology in systematics. In the case of the remaining skulls 1 to 4, there is also debate as to the number of species present (Scardia et al., 2021).

1.5 Choice of reference populations

A critical element of this study will be the choice of modern human reference populations for comparison with the Dmanisi skulls. These will be selected from the dataset of cranial measurements compiled by W. W. Howells which comprises 28 human populations covering all major geographic areas. The methodology and selected reference populations will have a direct impact on the strength of arguments this study brings to the above debate.

2 MATERIALS AND METHODS

Figure 1. *Location of Dmanisi in the Georgian Caucasus. Reproduced from Gibbons, 2013.*

2.1 The Dmanisi crania

Over a period of six years from 1999 to 2005, five crania were uncovered by the excavations at Dmanisi. Additionally, the site has yielded four mandibles, the first of which was found in 1991. The mandibles have been successfully associated with four of the crania, complementing the information and conclusions of research on the hominins. Figure 4 summarises the information on each of the skulls which will be reviewed below.

Skulls 1 and 2

These two crania were uncovered in 1999 in Block 1. Skull 1 is an almost complete calvaria, whereas skull 2 is a more complete cranium, retaining a large part of the face and cranial vault (Gabunia, Vekua, Lordkipanidze, et al., 2000). Skull 1 has the largest endocranial capacity (730 cm^3) of the five Dmanisi crania and its flattened glabella and low parietal eminence above the border with the temporal squama indicate it could represent a large adult female (Rightmire et al., 2019).

Skull 2 has a smaller endocranial capacity of approximately 650 cm^3 and is associated with mandible D211 on the basis of the orientation and wear of the occlusal facets of the cheek teeth. The thinner brow, small mastoid process and smooth occiput of skull 2, together with the gracile nature of its associated mandible indicate that it is likely to be a young adult female (Rightmire et al., 2006).

Despite their small endocranial capacities, these two skulls were initially considered as displaying more affinities with *H. ergaster* than with *H. erectus*. This first occurrence of *H. ergaster* in northern latitudes far from Africa implied that the species was perhaps not just a simple geographic variant of *H. erectus* (Gabunia, Vekua, Lordkipanidze, et al., 2000). However, with the discovery of the fourth crania, it was considered that the attributes displayed by the vault, cranial base and facial skeleton of the then four-skull Dmanisi hominin assembly were more characteristic of *H. erectus,* with certain traits being only shared with Far Eastern populations of that species (Lordkipanidze et al., 2006).

Skull 3

Discovered in 2001, this cranium labelled D2700 was associated with mandible D2735, found close by, on the basis of the good fit of the cranium to the jaw when upper and lower tooth rows were placed in occlusion. The maxillary M3 teeth are partly erupted, leading to the conclusion that the individual is subadult. Though the skull exhibits the gracile morphology of a female, the large

Figure 2. *The Dmanisi crania, from left to right: Skull 1 (D2280), Skull 2 (D2282), Skull 3 (D2700), Skull 4 (D3444), and Skull 5 (D4500). Reproduced from Scardia et al., 2021.*

crowns and roots of the upper canines are indicative of masculinity, and hence the sex of skull 3 remains undetermined (Vekua et al., 2002).

The endocranial volume of skull 3 of 601 cm^3 is smaller than that of skulls 1 and 2, and further facial and cranial growth of this subadult might have resulted in parameters closer to the adult hominins at Dmanisi (Rightmire et al., 2019). Though the endocranial volume is near the mean for *H. habilis*, the similarities of D2700 with specimens from West Turkana or Koobi Fora lead the to the assignment of "the new skull provisionally to Homo erectus (=ergaster)" (Vekua et al., 2002).

Skull 4

Discovered in 2002, the adult and edentulous skull D3444 exhibits extensive bone loss due to resorption, as does the toothless mandible associated with it, D3900, which was uncovered one year later. Presenting an endocrinal volume of 641 cm^3, the skull presents more features of masculine morphology that the other 3 skulls discovered prior to it. As we have seen above, it was attributed to *Homo erectus* with traits shared by examples of that species from Java (Lordkipanidze et al., 2006).

Figure 3. *Lateral and occlusal views of three Dmanisi mandibles mentioned in the text. Reproduced from Rightmire et al., 2019.*

Skull 5

This cranium, specimen D4500, was found in 2005 and was associated with mandible D2600 uncovered in 2000. Despite having a large and prognathic face, the endocranial volume of skull 5 is 546 cm^3 - the lowest of all the Dmanisi hominins. The skull was considered male on the basis of its more prominent and massive cranial superstructures when compared to the other Dmanisi hominins (Lordkipanidze, De Ponce León, et al., 2013).

In their research article on skull 5, the authors propose that specimens generally assigned to *H.*

ergaster could be attributed to a chrono-subspecies *H. erectus ergaster* given the limited number of samples available from the archaeological record. The Dmanisi population possibly had its origin in a dispersal out of Africa of the *Homo erectus* lineage and so it could be placed within that same *H. erectus ergaster* classification. Reference to geographic location was added to the designation so as to give the deme's final classification of *H. erectus ergaster georgicus* (Lordkipanidze, Ponce de León, et al., 2013).

	Skull 1	Skull 2	Skull 3	Skull 4	Skull 5
Specimen number	D2280	D2282	D2700	D3444	D4500
Date of find	1999	1999	2001	2002	2005
Associated mandible		D211	D2735	D3900	D2600
Find location	Block 1	Block 1	Block 2	Block 2	Block 2
Age	Adult	Young adult	Subadult	Old adult	Adult
Sex	Possible female	Female	Undetermined	Male	Male
Endocranial volume cm^3	730	650	601	641	546

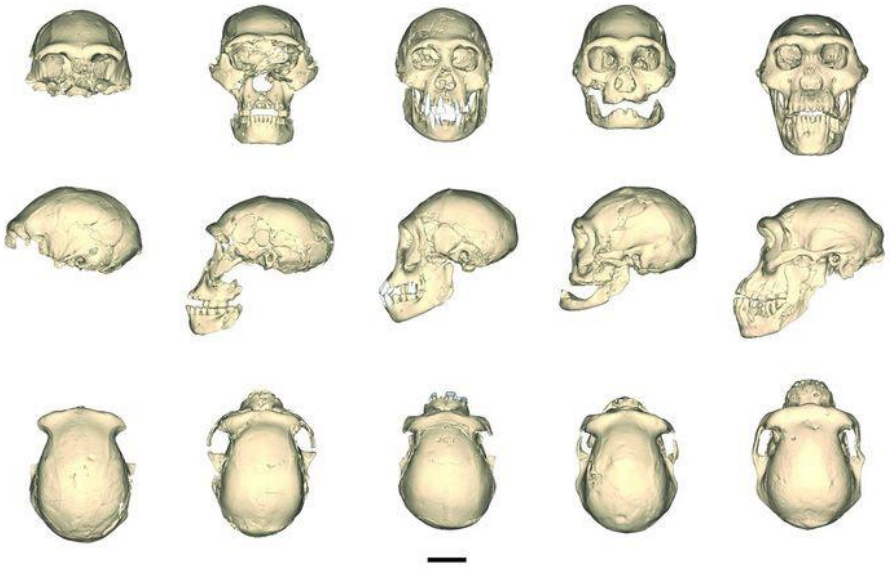

Figure 4. *The five Dmanisi crania with data of specimen numbers, find date and location, age, sex and cranial volume. Scale bar indicates 50 mm. Computer tomography scan reproduced from Lordkipanidze, De Ponce León, et al., 2013*

2.2 Hominin fossils constrained by dating and proximity

The basalt underlying the layers where the Dmanisi human remains were found has been dated by 40Ar/39Ar to 1,85 Mya (million years ago). The basalt and stratum A directly overlaying it have a normal geomagnetic polarity corresponding to the end of the Olduvai Subchron, whereas all of stratum B which contains the hominin remains, has a reversed polarity, dated to the Upper Matuyama chron at approximately 1,77 Mya (Ferring et al., 2011).

In Block 1 the hominin remains were contained in the single layer formerly denoted with the roman numeral V (Gabunia, Vekua, Lordkipanidze, et al., 2000) but in Block 2 they were contained within three of the subunits of stratum B formed by a process that included ashfalls and cycles of

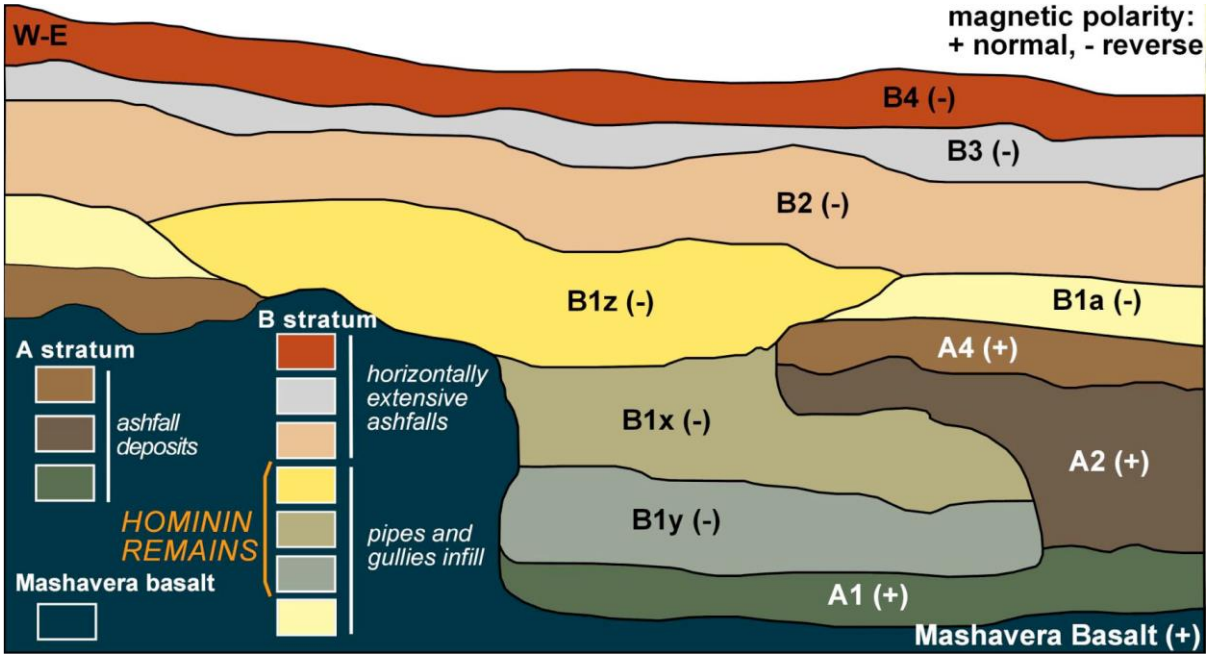

Figure 5. *Block 2 stratigraphic units. Skulls 3 and 4 were found in unit B1x. Skull 5 was uncovered in unit B1y. Reproduced from the Supplementary Information to Lordkipanidze et al., 2007.*

subterranean piping, gully formation and filling. (Lordkipanidze et al., 2007). Based upon the basalt weathering rate, it is estimated that the hominin bearing sediments were deposited and sealed in less than ten thousand years. This is further evidenced by the intact taphonomic condition of the fossils and their physical and microstratigraphic proximity (Lordkipanidze et al., 2006).

The evidence of a rapid accumulation and burial of the hominin remains is further supported by the stratigraphic correlation of the Dmanisi sediments with the Orozmani Basalt 15 km away and which was dated to 1,76 Mya (Gabunia, Vekua, Lordkipanidze, et al., 2000). Dmanisi could therefore have been occupied repeatedly over a period of 80.000 years with a sustained regional population (Ferring et al., 2011).

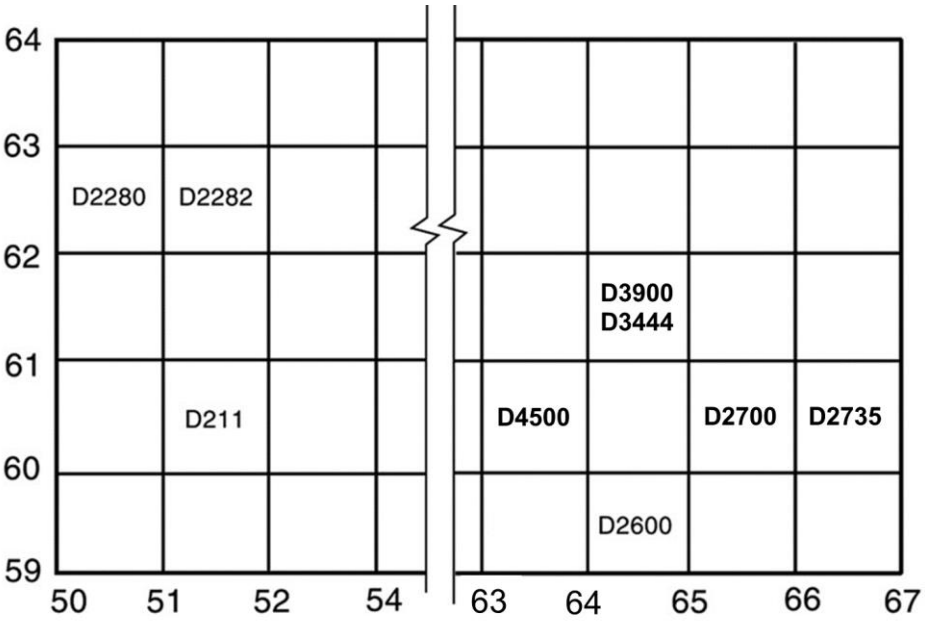

Figure 6. *The location of each hominin fossil described in Figure 4. The excavation units are 1 metre squares. The top of the quadrant faces North. Modified from Vekua et al., 2002*

As can be seen from Figure 6, The Dmanisi crania were all discovered in a radius of less than 10 metres. The close proximity of the remains is a further robust constraint on top of the dating constraint seen above. When viewed together, they contribute to the single taxon interpretation of the Dmanisi remains (Van Arsdale & Lordkipanidze. 2012).

2.3 Description of Howells dataset and some of its applications

The reference data of measurements of *Homo sapiens* skulls that we use for comparison with the measurements of the Dmanisi skulls was compiled by W. W. Howells over the course of 15 years from 1965 to 1980. 57 standardised measurements were taken from 2504 skulls representing 28 specific populations covering all major geographic regions (Howells, 1996). Table 13 presents a summary of the skulls by sex and population group.

Several aspects of the dataset make it particularly useful for the analysis that will be performed:

1. the populations were chosen by Howells with a view to investigating local differentiation in human skull variations before the 1492 discovery of the Americas and before the expansion of European populations worldwide with its related impact on the ancestry of local populations;

2. a further primary objective was that each series of skulls should represent a geographically confined population unit within a defined time span, limiting possible intra-group variation caused by climatic factors;

3. defining the sex of each skull was an important aspect of the study. 1348 of the specimens were known (from dissecting room collections) or diagnosed as male, and the remaining 1156 were similarly known or diagnosed as female;

4. finally, for the subsequent quantitative analyses that he would perform, Howells determined that each series of skulls should be represented by at least 27 individuals of each sex. Of the 28 populations that make up the dataset, two are composed of only males, and one has just 18 members of one sex (Howells, 1989). Neither of these three groups were chosen for subsequent analysis in this current study.

The Howells dataset was compiled in a systematic and consistent manner by a single highly qualified researcher, documenting the reasoning behind his choices of skulls for each population. In addition to being used for research purposes such as that presented here, the dataset is also used by computer programmes such as FORDISC to provide forensic investigators with an estimation of the sex and ancestry of unknown human remains.

FORDISC was recently used along with isotope analysis to confirm the diverse ancestry of the crew of the Tudor warship *Mary Rose* which sank off the British coast in 1545 (Scorrer et al., 2021). The programme was also used along with mtDNA sequencing to confirm the European ancestry of skeletal remains found at an Indian burial site in Texas, possibly confirming the individual to be a member of La Salle's last expedition in 1687 (Ambers et al., 2021).

The Howells dataset is made available for download at https://web.utk.edu/~auerbach/HOWL.htm where two datasets are available, as described in Howells, 1996. Before using the data from the HOWELL.XLS file in the analyses in this document, calculations were performed on the data, reproducing a sample of the statistics published in Howells, 1989. The results of these calculations are documented in Table 5 and confirm the accuracy and completeness of the data we will later use.

2.4 Description and visual representation of cranial measurements analysed

The following 10 craniometric measurements are used in the analysis, five of them corresponding to the braincase, and five of them corresponding to the facial skeleton:

Braincase		Facial skeleton	
Description	Howells abbreviation	Description	Howells abbreviation
Glabello-occipital length	GOL	Biorbital chord	FMB
Porion-vertex height	VRR	Bimaxillary chord	ZMB
Max. cranial breadth	XCB	Cheek height	WMH
Biauricular breadth	AUB	Max. malar height	XML
Biasterionic breadth	ASB	Nasal breadth	NLB

Table 1. *Craniometric measurements analysed in this study*

The above descriptions of the cranial measurements were used in published research on the Dmanisi hominis (Rightmire et al., 2017, 2019). To confirm the correct correspondence with the abbreviations and data published by Howells, 1989 the coefficient of variance (CV) for the 283 Africa population of Table 3 from Rightmire et al., 2019 was recalculated.

			This paper			Table 3
Measurement description	**Abb**	**n**	$\overline{X}$	**SD**	**CV**	**CV**
Glabello-occipital length	**GOL**	283	178,1	7,62	4,3	4,3
Porion-vertex height	**VRR**	283	119,0	4,76	4,0	4,4
Max. cranial breadth	**XCB**	283	132,1	5,76	4,4	4,4
Biauricular breadth	**AUB**	283	113,7	4,36	3,8	3,8
Biasterionic breadth	**ASB**	283	102,9	4,57	4,4	4,4
Biorbital chord	**FMB**	283	98,1	4,23	4,3	4,3
Bimaxillary chord	**ZMB**	283	94,7	5,16	5,5	5,5
Cheek height	**WMH**	283	20,6	2,27	11,0	11,0
Max. malar height	**XML**	283	51,9	3,74	7,2	7,2
Nasal breadth	**NLB**	283	28,0	1,84	6,6	6,6

Table 2. *Recalculation of the CV for the pooled samples of 283 Dogon, Teita and Zulu crania used in Table 3 by* Rightmire et al., 2019*. Average and standard deviation in mm.*

Nine of the ten calculated CV's resulted in the same value as previously published, confirming the correct selection of the corresponding Howells measurements. As a result of the difference highlighted above in calculated (4,0) and published (4,4) Porion-vertex height for the pooled sample of 283 Africa crania, the definition of this measurement was reviewed.

In the Supplementary Online Material published by Rightmire et al., 2017, Table S1 Measurement definitions states: "Porion-vertex height - cranial height as calculated from ½ of the biporionic diameter and the chord from porion to vertex, following Bräuer (1988)". The reference to Bräuer, 1988 is assumed to refer to calculating the height from porion to vertex as the unknown side of a right-angled triangle using Pythagoras' theorem. This unknown side is the thick red line in Figure 8 below and corresponds to the VRR measurement proposed by Howells. The choice of the VRR measurement is correct in this case, and the difference in the coefficient of variances observed above might arise due to computation, rounding protocols or a typing mistake.

Glabello-occipital length - GOL

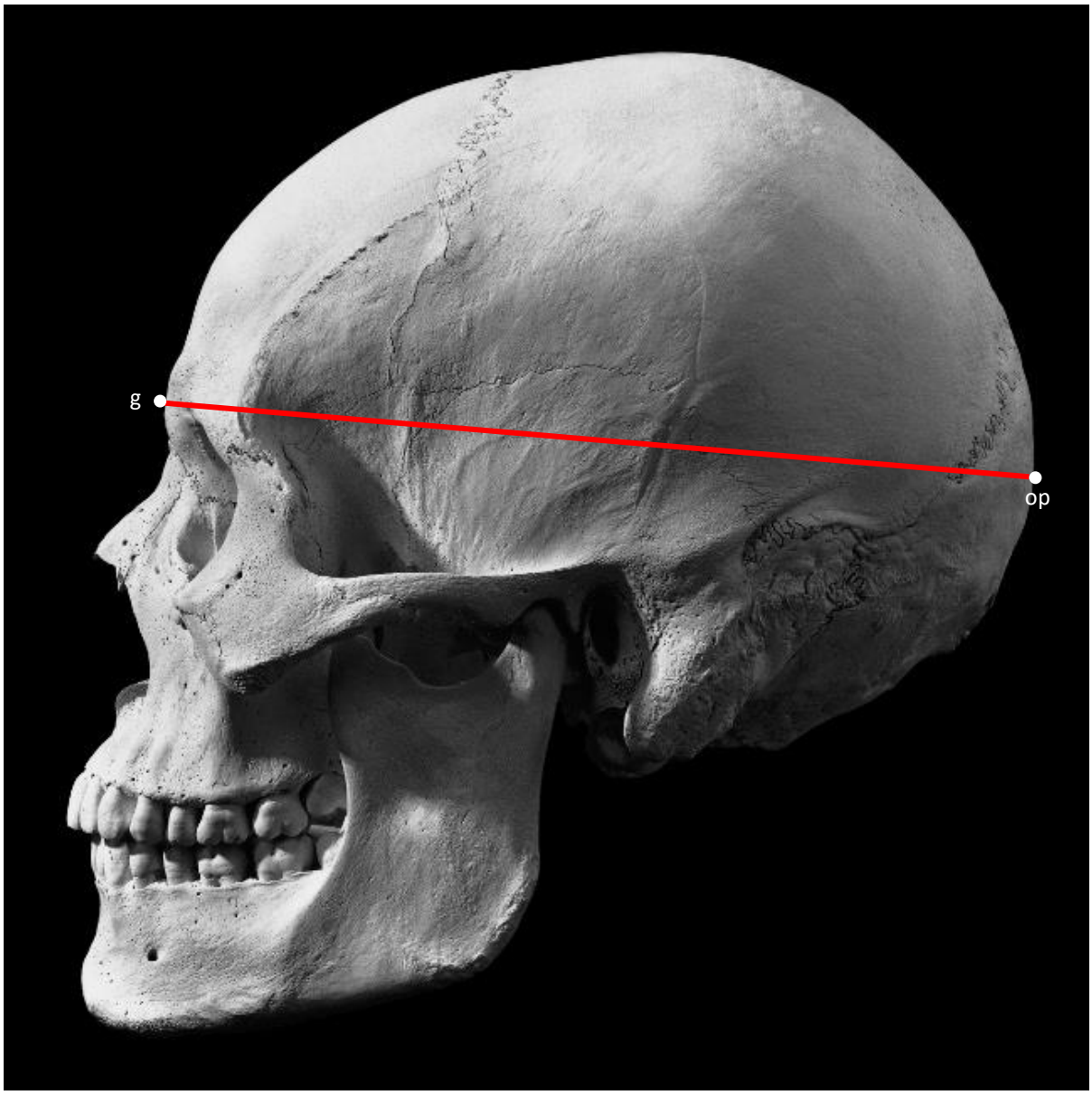

Figure 7. *(modification of picture taken from White et al., 2012)*

This measurement is often referred to as cranial length

Measurement definition (Howells, 1989)

Greatest length, from the glabellar region, in the median sagittal plane

Landmarks (definition reproduced from White et al., 2012)

g: Glabella is the most anterior midline point on the frontal bone, usually above the frontonasal suture

op: Opisthocranion is an instrumentally determined point at the rear of the cranium. It is defined as the midline ectocranial point at the farthest chord length from glabella

Porion Vertex Height – VRR

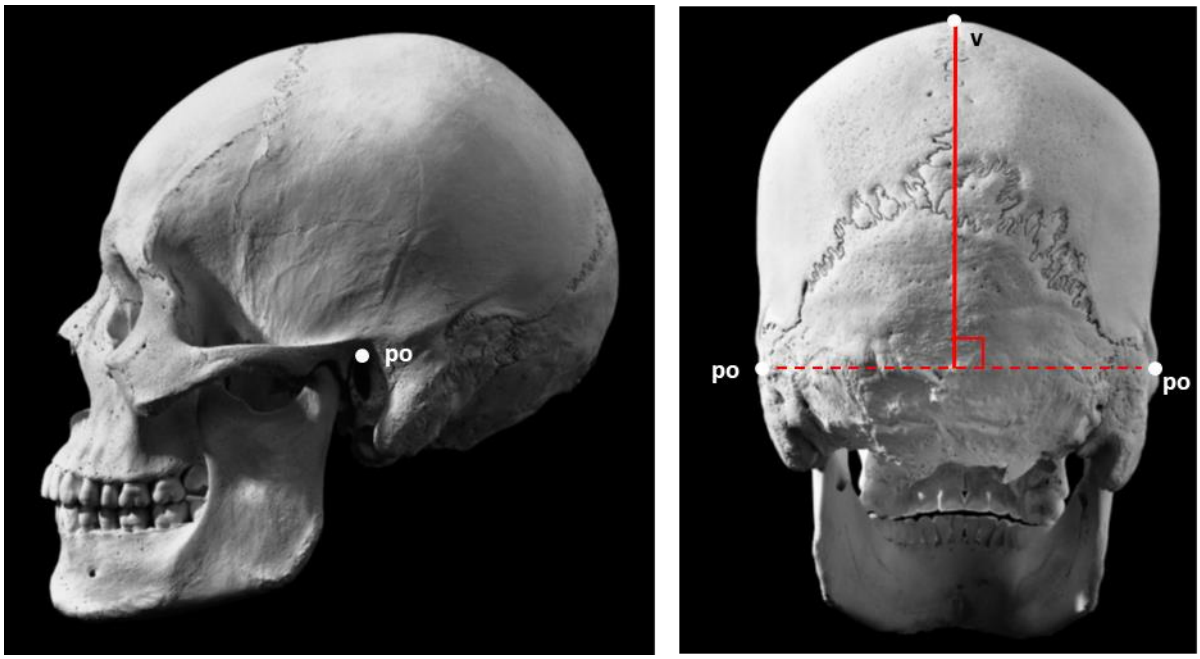

Figure 8. *(modification of picture taken from White et al., 2012) The thick red line represents the VRR measurement.*

This measurement can also be found described as cranial height. Howells described it as "Vertex radius"

Measurement definition (Howells, 1989)

The perpendicular to the transmeatal axis from the most distant point on the parietals (including bregma or lambda), wherever found.

Landmarks (definition reproduced from White et al., 2012)

po: porion is the uppermost point on the margin of the external acoustic meatus.

v: vertex is determined instrumentally when the skull is in Frankfurt Horizontal. It is the highest ectocranial point on the skull's midline.

Maximum cranial breadth - XCB

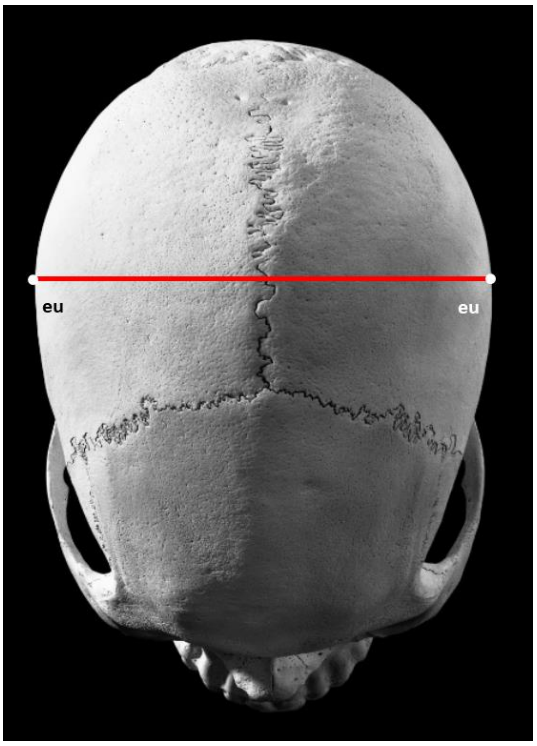

Figure 9. *(modification of picture taken from White et al., 2012)*

Measurement definition (Howells, 1989)
The maximum cranial breadth perpendicular to the median sagittal plane (above the supramastoid crests.

Landmarks (definition reproduced from White et al., 2012)

eu: Euryon is the instrumentally determined ectocranial point of greatest cranial breadth.

Biauricular breadth - AUB

Figure 10. *(modification of picture taken from White et al., 2012)*

Measurement definition (Howells, 1989)
The least exterior breadth across the roots of the zygomatic process, wherever found.

Biasterionic breadth- ASB

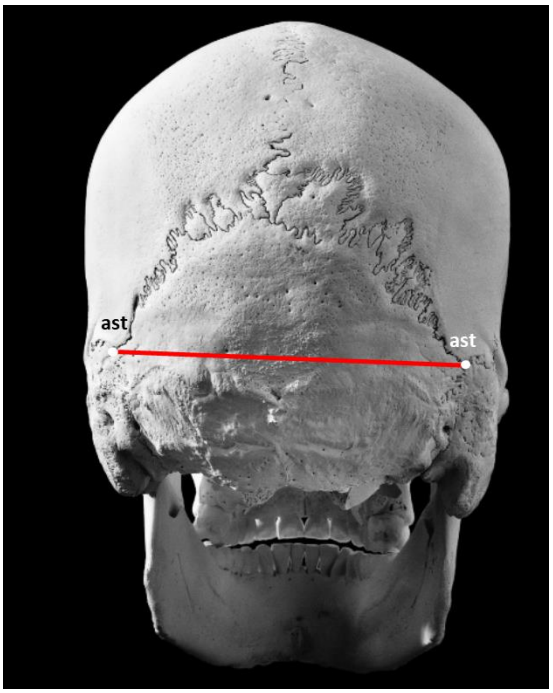

Figure 11. *(modification of picture taken from White et al., 2012)*

Measurement definition (Howells. 1989)
Direct measurement from one asterion to the other

Landmarks (definition reproduced from White et al., 2012)

ast: Asterion is the point where the lambdoid, parietomastoid, and occipitomastoid sutures meet

Biorbital chord - FMB

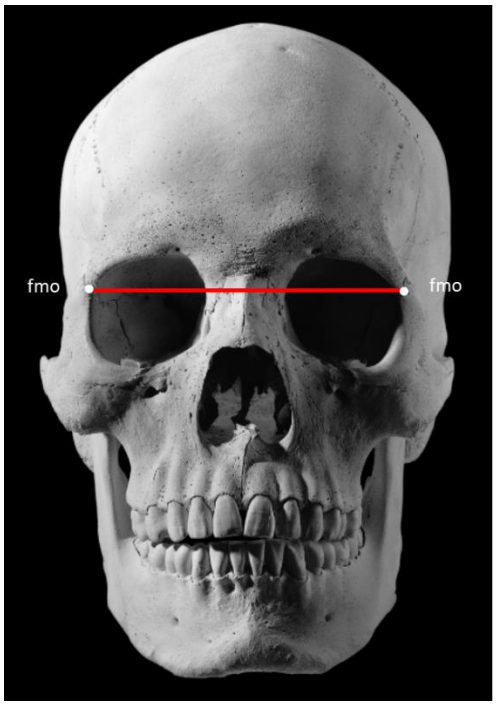

Figure 12. *(modification of picture taken from White et al., 2012)*

Howells described this measurement as "Bifrontal breadth"

Measurement definition (Howells, 1989)
The breadth across the frontal bone between frontomalare anterior on each side, ie, the most anterior point on the fronto-malar suture

Landmarks (definition reproduced from White et al., 2012)

fmo: Frontomalare orbitale is the point where the frontozygomatic suture crosses the inner orbital rim.

Bimaxillary chord - ZMB

Figure 13. *(modification of picture taken from White et al., 2012)*

Howells defines this measurement as "Bimaxiliary breadth"

Measurement definition (Howells. 1989)
The breadth across the maxillae, from one zygomaxillare to the other

Landmarks (definition reproduced from White et al., 2012)

zm: Zygomaxillare is the most inferior point on the zygomaticomaxillary suture.

Cheek height - WMH

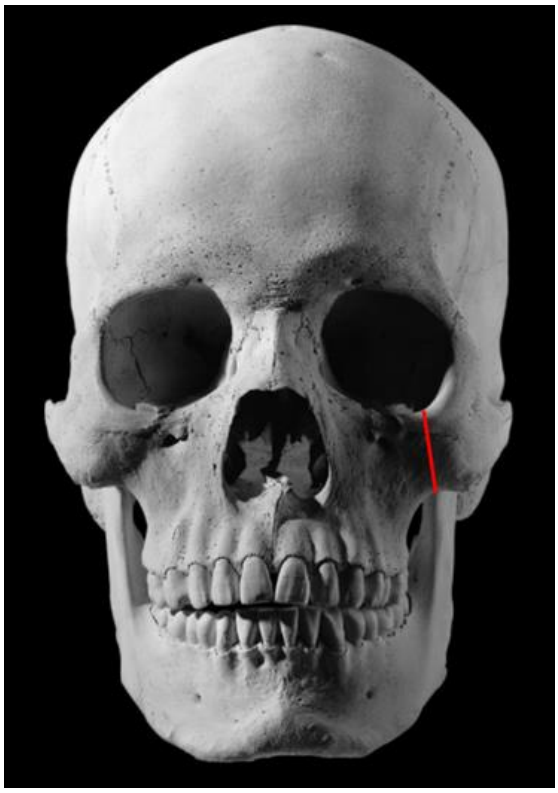

Figure 14. *(modification of picture taken from White et al., 2012)*

Measurement definition (Howells, 1989)
The minimum distance, in any direction, from the lower border of the orbit to the lower margin of the maxilla, mesial to the masseter attachment, on the left side.

It should be noted that this measurement is not necessarily a vertical measurement, as confirmed by the following comment in Howells, 1973: "Note: This differs from Martin´s "Wangenbeinhöhe," 48(4), which specifies measurement in a vertical direction."

Maximum malar height - XML

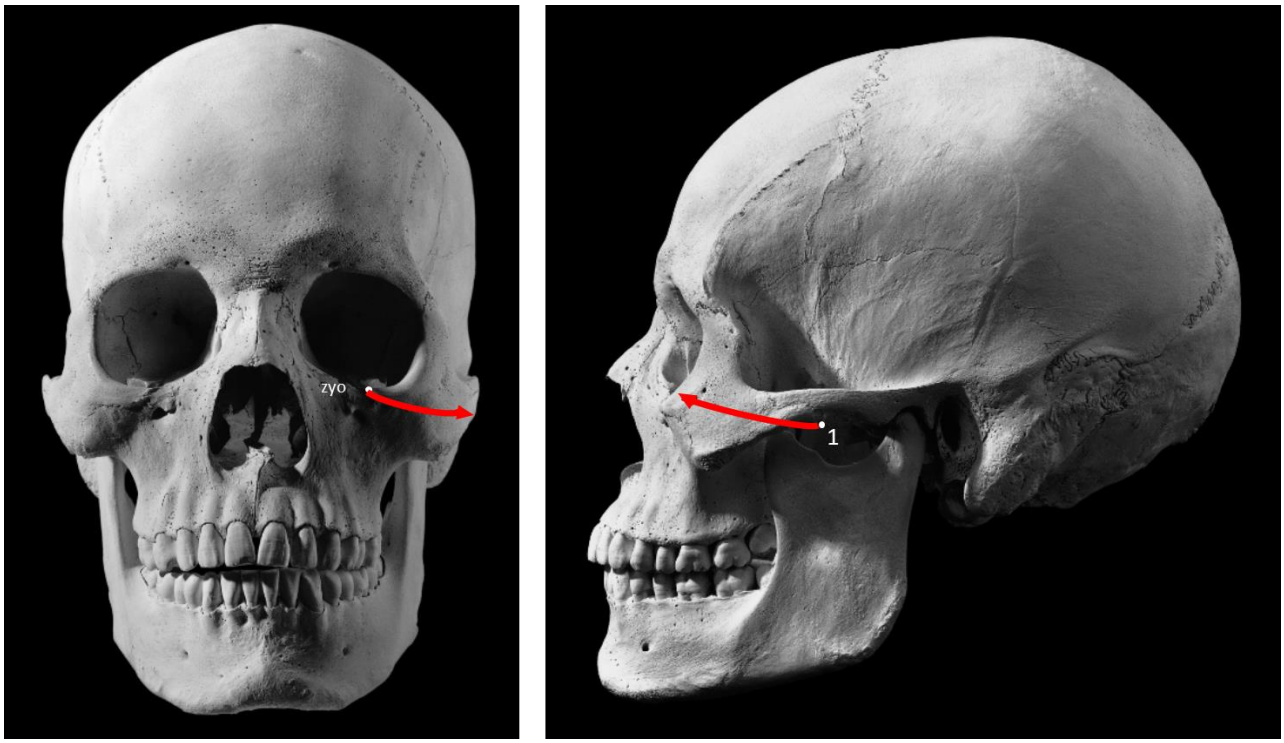

Figure 15. *(modification of picture taken from White et al., 2012)*

Howells refers to this measurement as Malar length, maximum

Measurement definition (Howells, 1989)

Total direct length of the malar in a diagonal direction, from the lower end of the zygotemporal suture on the lateral face of the bone, to zygoorbitale, the junction of the zygomaxillary suture with the lower border of the orbit, on the left side.

Landmarks (definition reproduced from White et al., 2012)

zyo: Zygoorbitale is the point where the orbital rim intersects the zygomaticomaxillary suture.

Other landmarks

1: lower end of zygotemporal suture

Nasal breadth - NLB

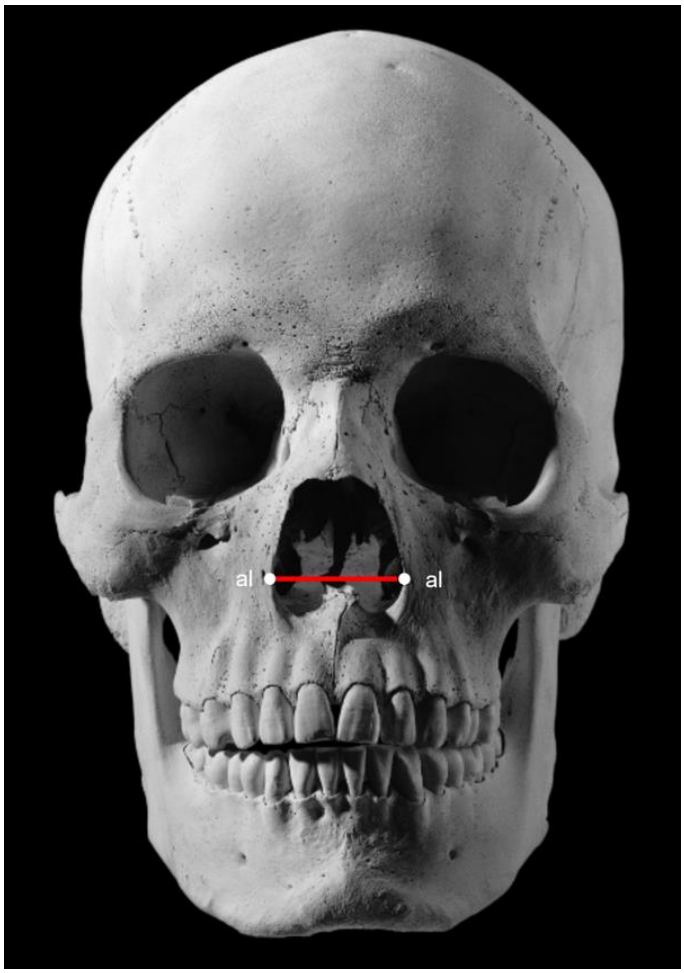

Figure 16. *(modification of picture taken from White et al., 2012)*

Measurement definition (Howells, 1989)

The distance between the anterior edges of the nasal aperture at its widest extent

Landmarks (definition reproduced from White et al., 2012)

al: Alare is instrumentally determined as the most lateral point on the margin of the anterior nasal aperture.

2.5 Dmanisi measurements

Table 3 presents the published measurement data for the Dmanisi skulls with their corresponding Howells measurement abbreviation.

Measurement description	Abbreviation	Skull 1	Skull 2	Skull 3	Skull 4	Skull 5
Glabello-occipital length	**GOL**	177		155	163	169
Porion-vertex height	**VRR**	91		77	82,5	73
Max. cranial breadth	**XCB**	136		126	132	135,5
Biauricular breadth	**AUB**	132		119	120	129
Biasterionic breadth	**ASB**	104	103	105	104	93
Biorbital chord	**FMB**		96	90	98	102
Bimaxillary chord	**ZMB**		91	97	93	110
Cheek height	**WMH**		30	28	25	30
Max. malar height	**XML**		43,5	39	40	44,5
Nasal breadth	**NLB**		27	28	28	31

Table 3. *The ten skull measurements for the Dmanisi crania as extracted from Tables 3 and 4 of* Rightmire et al., 2017. *Values expressed in mm.*

Skull 1 is a calvaria and hence it offers no values for the facial skeleton. In the case of skull 2, this fossil presented damage to the facial, occipital and zygomatic regions in addition to suffering post-mortem deformation (Gabunia, Vekua, Lordkipanidze, et al., 2000) and this accounts for the lack of four cranial measurements.

As a check of the accuracy of the data presented in Table 3, the coefficient of variance for the Dmanisi fossils presented in Table 3. of Rightmire et al., 2019 was recalculated in Table 4 below.

			This paper			Table 3
Measurement description	**Abb**	**n**	$\overline{X}$	**SD**	**CV**	**CV**
Glabello-occipital length	**GOL**	4	166,0	9,31	5,6	5,6
Porion-vertex height	**VRR**	4	80,9	7,79	9,6	9,6
Max. cranial breadth	**XCB**	4	132,4	4,61	3,5	3,5
Biauricular breadth	**AUB**	4	125,0	6,48	5,2	5,2
Biasterionic breadth	**ASB**	5	101,8	4,97	4,9	4,9
Biorbital chord	**FMB**	4	96,5	5,00	5,2	5,2
Bimaxillary chord	**ZMB**	4	97,8	8,54	8,7	8,7
Cheek height	**WMH**	4	28,3	2,36	8,4	8,3
Max. malar height	**XML**	4	41,8	2,66	6,4	6,4
Nasal breadth	**NLB**	4	28,5	1,73	6,1	6,1

Table 4. *Recalculation of the CV for Dmanisi fossils presented in Table 3 by* Rightmire et al., 2019. *Average and standard deviation in mm.*

This step reveals a small difference of 0,1 in the CV calculated for cheek height – WMH. The raw measurement data used was accurately extracted, and the difference in this statistic, probably due to rounding, is not considered material to the analysis in this paper.

2.6 Howells measurements

The HOWELL.XLS FILE available for download from https://web.utk.edu/~auerbach/HOWL.htm is comprised of 2524 individuals (1368 males, 1156 females) a total which does not agree with Howells, 1989, being comprised of 2504 individuals (1348 males, 1156 females).

Inspection of the downloaded file revealed two additional population groups, labelled "N Maori" and" S Maori" composed of 10 male individuals each. The elimination of these 20 individuals yields the totals given in Howells, 1996. The total of females and male individuals for each of the 28 population groups given on page 2 of Howells, 1989 was also checked.

No checksum digits are available to detect possible errors in the online Howells data. To ensure the accuracy of the ten chosen measurements subsequently used in this paper, a series of published statistics from Howells, 1989 were recalculated. For 18 of the populations, the published mean of means was recalculated for 10 of the measurements. The mean of means statistic was not published for the other 10 populations, and the group standard deviation for one each of the 10 selected measurements was calculated in its place. Table 5 presents the statistics that were checked to published values and for which no discrepancy was found.

Description of population	Statistic checked	Abbreviation	Value calculated		Page number
			Males	Females	Howells, 1989
Groups 1 to 18	Mean of means	GOL	183,60	174,71	Page 10
Groups 1 to 18	Mean of means	XCB	138,47	133,64	Page 10
Groups 1 to 18	Mean of means	AUB	123,42	116,98	Page 10
Groups 1 to 18	Mean of means	ASB	108,58	104,21	Page 10
Groups 1 to 18	Mean of means	NLB	26,95	25,89	Page 10
Groups 1 to 18	Mean of means	ZMB	97,38	91,89	Page 10
Groups 1 to 18	Mean of means	FMB	99,49	94,74	Page 10
Groups 1 to 18	Mean of means	XML	54,62	50,48	Page 10
Groups 1 to 18	Mean of means	WMH	23,37	21,55	Page 10
Groups 1 to 18	Mean of means	VRR	122,99	118,19	Page 10
Group 19 Taiwan Aboriginals: Atayal	Standard deviation	GOL	5,81	4,54	Page 139
Group 20 Philippine Islands: General	Standard deviation	XCB	5,61		Page 140
Group 21 Guam: Latte Period	Standard deviation	AUB	4,19	3,99	Page 141
Group 22 Egypt: Gizeh, 26th-30th Dynasties	Standard deviation	ASB	4,43	4,55	Page 141
Group 23 South Africa: Bushman (San)	Standard deviation	NLB	2,27	2,10	Page 143
Group 24 Andaman Islands: General	Standard deviation	ZMB	3,98	3,78	Page 144
Group 25 Ainu, Japan: South and Southeast Hokkaido	Standard deviation	FMB	4,12	3,32	Page 144
Group 26 Sibeira: Buriats	Standard deviation	XML	3,43	3,39	Page 147
Group 27 Geenland: Inugsuk Eskimo	Standard deviation	WMH	2,14	2,30	Page 147
Group 28 Shang Dynasty Chinese: Anyang	Standard deviation	VRR	4,08		Page 150

Table 5. *Statistics recalculated to ensure accuracy of the data subsequently used in this paper. No discrepancy was found with published values (Howells, 1989).*

2.7 Description of bootstrapping

For researchers working in the field of palaeontology and human evolution, the statistical technique known as bootstrapping provides a powerful tool for comparing the mostly small fossil samples found in the archaeological record with the generally far larger reference samples developed from taxa present in the living world. The ability to make meaningful and quantifiable comparisons between fossil and living samples unlocks additional information that might render interpretation more challenging, but it does contribute to the strength of the conclusions that are made.

Bootstrapping is a statistical methodology that creates new samples by resampling with replacement from a population (Efron & Tibshirani, 1993). Thousands of randomly generated samples of size n, where n is the size of the fossil assemblage, can be generated from a large reference population, and statistics such as the coefficient of variation of the fossil sample can be meaningfully compared with the CV of the simulated samples given they have the same size (Lockwood et al., 1996).

Bootstrapping has been used in several studies, comparing fossil hominins with extant species. The technique was applied in a comparison of the mandibles, proximal femora and humeri of *Australopithecus afarensis* with humans, gorillas, orang-utans and chimpanzees (Lockwood et al., 1996). Whilst concluding that the sexual dimorphism of *A. afarensis* did not exceed that of gorillas and orang-utans, it did however conclude that the species was probably more variable in size than modern humans and chimpanzees.

A study of the cranial and postcranial remains of archaic humans uncovered at Sima de los Huesos (Lorenzo et al., 1998) used bootstrapping to compare the fossils with modern humans, rejecting the hypothesis of greater sexual dimorphism in this Middle Pleistocene group when compared to modern populations. A review of the body size, brain size, and sexual dimorphism of *Homo naledi* (Garvin et al., 2017) used bootstrapping in part of its analysis, concluding that the species had slight dental dimorphism and a sexual size dimorphism comparable to *H. sapiens.* These contrast however with features not typical of the *Homo* genus such as a small brain and small body.

Much of the published research uses specialised software to execute the bootstrapping technique. However, commercially available Microsoft Excel spreadsheets have a tabling function that allows for bootstrapping to be performed without specialised software (Hurley, 2000). All the bootstrapping calculations performed in this current research were performed on Excel 2019.

The Appendix details the steps for performing in Excel 2019 the bootstrapping calculations of the example given in Hurley, 2000.

3 RESULTS

3.1 Selection of a reference population

The choice of the Howells reference population or populations which will be used in the present analysis will have a direct impact on the strength of the conclusions obtained. The rationale behind the methodology adopted in this important step is explained below.

3.2 Considerations in selecting a reference population

Plavcan & Cope, 2001, reflect upon the selection method to be followed in the choice of a reference sample for comparison with a fossil sample and state that the question does not have an absolute answer. They indicate two possible criteria that could be followed: using ecological or morphological similarities to decide the choice of a reference population; or choosing an extreme reference population with the possible consequence of arriving at a conservative result. They additionally recommend limiting comparisons to restricted geographic and time horizons. Rightmire et al., 2019 also confirm the lack of guidelines in selecting reference populations and agree that they should be geographically restricted.

Based upon the foregoing review of guidelines published in the scientific literature, two categories of reference samples of modern humans will be prepared for comparison with the Dmanisi hominis. The conditions each sample must fulfil are described as follows.

Sample 1 – Ecological reference sample

The conditions that this sample of modern humans should satisfy are:

1. it should represent a localised population from a relatively short time frame (restricted geographic and time conditions)

2. include both males and females (morphological condition);

3. be located in an area with a comparable climate (ecological condition).

With regards condition 1 above - geographic and time restrictions - the choice of a sample will be guided by the information provided in Howells, 1989 concerning the source of each set of skulls measured, as briefly summarised in Table 13 below.

Condition 2 aims to account for possible dimorphism present in the Dmanisi skulls. As indicated previously, skull 1 is possibly female, skull 2 is considered female, and the sex of skull 3 cannot be determined. It is important therefore that the reference population includes both males and females. Of the 28 series of skulls measured in Howells, 1989 and summarized in Table 13, just 2 series are restricted to a single sex, and therefore our selection will be extracted from the remaining 26 groups.

Finally, to satisfy the ecological condition- 3 above - the paleoenvironment of Dmanisi at the time of the hominin occupation will be determined from a review of available literature. The updated Köppen-Geiger climate classification (Kottek et al., 2006) will be used to filter the Howells groups and find a reference population in an area with a climate similar to that of Dmanisi 1,8 Mya.

Sample 2 – Extreme reference sample

The second sample should represent two populations chosen for being at the extremes of the range of measurements used in Howells, 1989. We shall combine a population displaying generally smaller cranial measurements together with a population showing generally larger cranial measurements. This sample will then be used to analyse the Dmanisi sample.

If additionally, this sample 2 could also fulfil all of the conditions of sample 1, it would provide additional weight to the final conclusions of this analysis.

3.3 Preparation of an ecological reference population

We will determine in the following sections 3.4 to 3.7 the Dmanisi climate at 1,8 Mya, and then in section 3.7 establish which Howells populations lived in a similar climate.

3.4 Dmanisi climate at the time of hominin occupation

Several studies have revealed the paleoenvironmental conditions of Dmanisi at the time of the hominin occupation. We shall review a selection of these below.

A carpological study of the fossil fruits obtained from sieving the sediment found in association with the hominins yielded over 500 fruit remains. Two main fossil fruit groups were identified: the deciduous tree genus *Celtis* (n=3), and seven herbaceous taxa from the Boraginaceae family (n>500). The three fossilised fruits of the tree genus *Celtis* were assigned to *Celtis tournefortii,* the more drought resistant member of this genus which can be found as a shrub or small tree of less than 6 meters, growing in open rocky places or in the forest steppes of areas such as the Anatoli mountains (Messager et al., 2008).

Turning to the Boraginaceae fruit, the most common morphotype (n=316) was assigned to the species *Lycopsis cf. orientalis,* present in steppe formations and areas with 60% vegetal density. The second most common morphotype (n>200) was assigned to the genus *Myosotis* whose members are found in both dry habitats as well as forest edges or river-banks, and therefore could not yield any precise indication of the paleoenvironment. Three of the remaining morphotypes (n=2 each) could come from open steppe formations, one (n=9) is present in Mediterranean or semi-arid conditions, and the final morphotype (n=1) could not provide any further climatic insights. The authors concluded that the Dmanisi area was covered by low xerophilous plants and grasses during an arid episode when the hominis arrived (Messager et al., 2008)

Thanks to their abundance in the stratigraphy of Dmanisi, phytoliths have also provided data on the paleoenvironment and paleoclimate. Their analysis confirmed the presence of grasses in strata A and B and allowed for a water stress index to be prepared. This index indicates a shift towards increasing aridity at the base of stratum B where the hominin remains were found (Messager et al., 2010)

Palynological analysis performed on the Dmanisi sediments points to an environment dominated by grasses with steppe elements. Forest ecosystems are present but in the regional environment (Messager et al., 2010)

The micromammal remains found in association with the hominin remails are represented close to 75% by gerbils and hamsters present in warm steppe environments. Approximately 10% of the micromammals at Dmanisi are associated with a forest environment, and the remaining 15% is composed of a rodent found in different environments. The collection of micromammals uncovered at Dmanisi reflect a generally arid warm steppe environment (Agustí & Lordkipanidze, 2011).

The large mammal assemblage is composed more than 80% by deer, pointing to the presence of a forested habitat in the nearby mountainous areas. However, the presence of taxa such as the ostrich *Struthio dmanisensis* or the lagomorph *Ochotona cf. lagreli* do point to the presence of steppe conditions. The hominins lived near a lake or pond, occupying an open steppe and gallery forest mosaic environment. (Gabunia, Vekua, & Lordkipanidze, 2000).

The amphibian and reptile remains obtained during the excavations were also used as proxies to confirm the paleoenvironment. Six taxa were identified (number of remains NR= 118, minimum number of individuals MNI= 11) and given that they are not extinct, their present-day ecologies were used to reconstruct the paleoenvironment. The amphibian and reptile fossil remains indicate arid conditions, from steppe to open Mediterranean forest, with the presence of a permanent aquatic body (Blain et al., 2014).

The climatic and environmental conditions inferred by each of the above proxies is summarised in Table 6 below:

Proxy	**Climate**	**Environment**
Fossil fruits	Arid	Steppe, regional forest
Phytoliths	Increasing aridity	Steppe
Pollen	Arid	Steppe, regional forest
Micromammals	Arid, warm	Steppe
Large mammals	Dry	Steppe, regional forest
Herpetofauna	Arid	Steppe, Mediterranean forest

Table 6*. Paleoclimate and paleoenvironment of Dmanisi at the time of the hominin occupation as determined by each proxy*

3.5 Köppen-Geiger climate classification

The German scientist Wladimir Köppen proposed the first quantitative classification of world climate in 1900. Trained as a plant physiologist, he classified the world's climate into five vegetation groups, each denoted with a letter from A to E as follows:

Letter	Climate zone
A	Equatorial
B	Arid
C	Warm temperate
D	Snow
E	Polar

Table 7. *First letter of the Köppen climate classification*

A second letter in the classification system defines precipitation:

Letter	Description
W	Desert
S	Steppe
f	Fully humid
s	Summer dry
w	Winter dry
m	Monsoonal

Table 8. *Second letter of the Köppen climate classification, defining precipitation.*

Finally, if necessary, a third letter defines air temperature as seen in Table 9. The total number of climate classes that can occur are 31.

Letter	Description
h	Hot steppe / desert
k	Cold steppe / desert
a	Hot summer
b	Warm summer
c	Cool summer & cold winter
d	Extremely continental
F	Polar frost
T	Polar tundra

Table 9. *The letter of the Köppen climate classification that defines air temperature.*

Various authors published enhanced editions of Köppen's original climate classification map, the most widely used version being developed by Rudolf Geiger in 1961. An updated and more precise version of the Köppen-Geiger climate classification map has been produced, combining two sets of data, one for temperature and one for precipitation, on a 0.5 degree latitude/longitude grid with monthly climate data for the 50 year period 1951 to 2000 (Kottek et al., 2006).

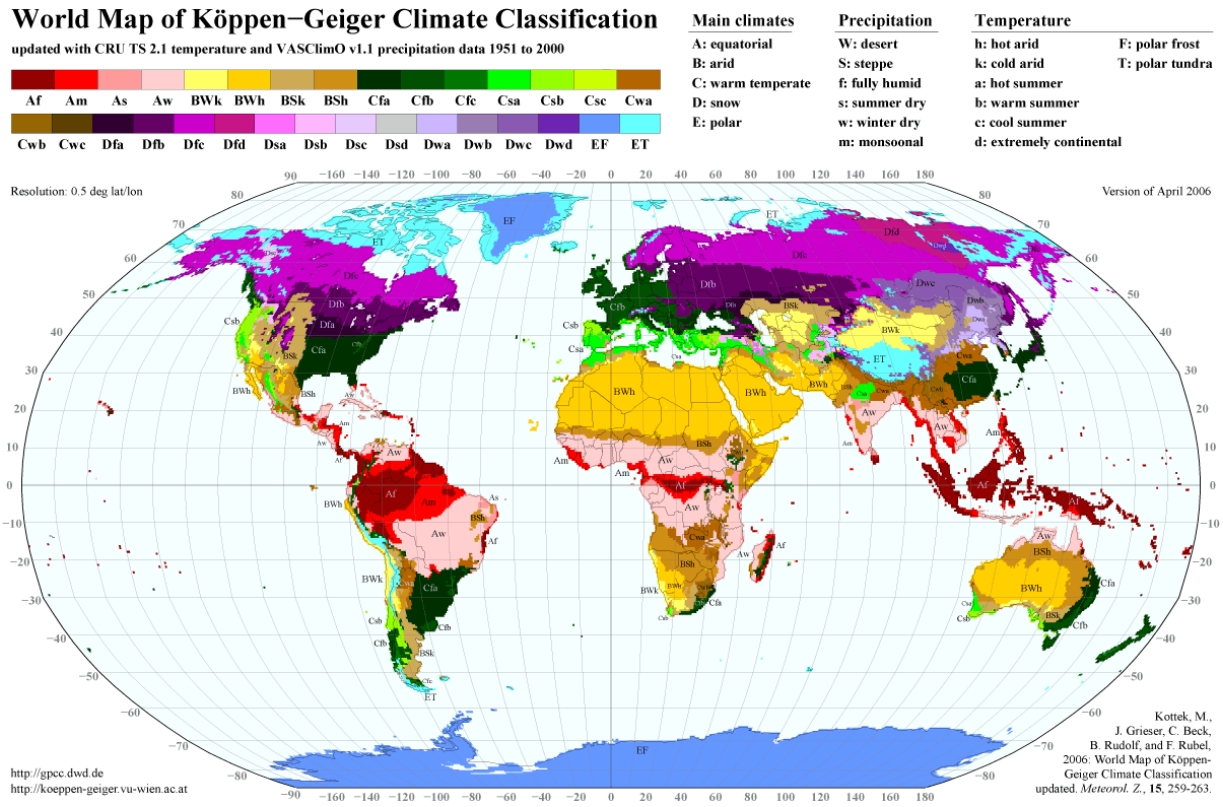

Figure 17. *World Map of Köppen-Geiger climate classification elaborated with data for the period 1951 to 2000 (Kottek et al., 2006).*

3.6 Choosing one or more Köppen-Geiger climate classifications

An initial review of Table 6, the Dmanisi paleoclimate and paleoenvironment determined by each proxy, would indicate that for the past climate of Dmanisi, our choices for the first two letters of the Köppen-Geiger classification would be:

B Arid (from Table 7 – Climate zone)

S Steppe (from Table 8 - Precipitation)

The final letter has two possible choices as indicated in Table 9 – air temperature:

h Hot steppe / desert

k Cold steppe / desert

Referring to the data in Figure 17, the two climate zones are therefore BSh and BSk.

The criteria for choosing between either of these choices depends upon temperature. Hot steppe is defined as having a mean annual surface temperature equal to or in excess of 18 °C, and cold steppe is defined as having that same mean under 18 °C. The qualitative data we have complied above

from proxies does not give any evidence to decide between either temperature parameter, and thus both shall be used in the analysis of the Howells populations.

The herpetofauna study indicated above used the mutual climatic range (MCR) method to estimate values for mean annual temperature and mean annual precipitation (Blain et al., 2014). The above qualitative interpretation can therefore be compared for reasonableness with quantitative data calculated on the following basis:

	Mean annual temperature in °C (MAT)	Mean annual precipitation in mm (MAP)
Mean	13,1	635
Standard deviation	2,4	191

Table 10. *Data extracted from Table 2 in (Blain et al., 2014).*

To confirm our choices of climate zones BSh and BSk we need to confirm that the following conditions are satisfied:

BS Steppe climate $5\ P_{th} < P_{ann} < 10\ P_{th}$

where P_{ann} is defined as the accumulated annual precipitation and P_{th} is defined as:

$$P_{th} = \begin{cases} 2\{T_{ann}\} & \text{if at least 2/3 of the annual precipitation occurs in winter,} \\ 2\{T_{ann}\}+28 & \text{if at least 2/3 of the annual precipitation occurs in summer,} \\ 2\{T_{ann}\}+14 & \text{otherwise.} \end{cases}$$

Figure 18. *Formula reproduced from Kottek et al., 2006*

where T_{ann} is defined as the annual mean near-surface (2 metre) temperature.

The definition of winter for the purposes of the formula in Figure 18 is the six months from October to March. This monthly data is not available in Blain et al., 2014 so we will assume that 2/3 of the annual precipitation occur in winter, the most stringent of the three criteria in the formula.

The original condition for the BS steppe climate above:

BS Steppe climate $5\ P_{th} < P_{ann} < 10\ P_{th}$

therefore becomes:

BS Steppe climate $5 \times (2\ T_{ann}) < P_{ann} < 10 \times (2\ T_{ann})$.

Inserting MAT for $T_{ann\ and}$ MAP for P_{ann} in the above equation we obtain:

Average : $5 \times (2 \times 13{,}1) < 635 < 10 \times (2 \times 13{,}1)$

$131 < 635 < 262$ **False**

Reducing precipitation by 1 standard deviation (SD), and increasing temperature by 1 SD we obtain:

1 SD : $5 \times (2 \times (13{,}1+2{,}4)) < 635-191 < 10 \times (2 \times (13{,}1+2{,}4))$

131 < 444 < 262 **False**

Reducing precipitation by 1,6 SD, and increasing temperature by 1,6 SD we obtain:

1,6 SD : 5 x (2 x (13,1+(2,4 x 1,6))) < 635 - (191 x 1,6) < 10 x (2 x (13,1+(2,4 x 1,6)))

169 < 329 < 339 **True**

Though the probability of these two independent parameters for temperature and precipitation having the above 1,6 SD variation together is small, it is nevertheless a possibility. This quantitative data does not exclude the conclusions arrived at by qualitative means.

Further quantitative research using dental ecometric variables of fossil ungulates has provided additional mean temperature and precipitation data for Dmanisi (Saarinen et al., 2021), indicating both higher temperatures and lower precipitation values at Dmanisi than those quoted above. An updated study of the same Dmanisi herpetofauna, using more precise universal transverse Mercator grids, the uncertain distribution area-occupied distribution area (UDA-ODA) discrimination technique and the mutual ecogeographic range (MER) method (similar to the prior MCR) also yielded a higher temperature but significantly more precipitation (Blain et al., 2022).

Proxy	Method	Mean annual temperature in ^{o}C (MAT)	Mean annual precipitation in mm (MAP)	Reference
Herpetofauna	MCR	13,1	635	Blain et al., 2014
Ungulates	Dental ecometrics	16,9	453	Saarinen et al., 2021
Herpetofauna	MER and UDO-UDA	16,2	725	Blain et al., 2022

Table 11. *Summary of published quantitative temperature and precipitation data for Dmanisi*

As can be seen from Table 11, the two recent studies show a relatively small difference in mean annual temperature (0,7 degrees) but a larger and more significant difference in mean annual precipitation (272 mm). These differences could be due to the geographic configuration of Dmanisi at the time of the hominin occupation when it is estimated to have been just 60 km from the Caspian Sea versus 400 km at present. Additionally, the strong precipitation seasonality detected in the most recent herpetofauna quantitative data, with negligible rainfall from June to September, might have impacted to a greater extent the dental ecometric signal of the ungulate population (Blain et al., 2022).

The differences in mean annual temperature and mean annual precipitation of the two proxies summarised in Table 11 are such that they do not provide a basis for invalidating the qualitative interpretation of the other proxies. Instead, those studies should be considered as providing evidence for widening the potential climate filter we seek to apply. The updated herpetofauna study produced monthly temperatures for Dmanisi and on this basis provided a Mediterranean-type climate classification Csa – warm temperate climate with dry and hot summer (Blain et al., 2022).

In conclusion, the following climate filters will be applied to the 28 Howells populations:

Köppen-Geiger Climate	Description
Csa	Warm temperate climate, dry and hot summer
BSk	Cold steppe
BSh	Hot steppe

Table 12. *Summary of climate filters chosen in this study*

In choosing the classifications indicated in Table 12, we are effectively including representative climates from both sides of the debate on the type of environment present at the time of the early hominin dispersal out of Africa. Our inclusion of hot and cold steppes reflects the "savannastan" hypothesis (Dennell & Roebroeks, 2005), whereas the inclusion of the Mediterranean climate category Csa acknowledges the alternative woodland hypothesis (Belmaker & O'Brien, 2018).

3.7 Defining the climate classification of the 28 Howells populations

The next step in the analysis is to define the Köppen-Geiger climate for each of the 28 Howells populations. To do this, Appendix A of Howells, 1989 has been used as this describes the source and composition of each series of skulls, providing information to confirm the geographic location of each population.

For the climate classification of the geographic locations defined above, the online weather database https://en.climate-data.org was used. This website uses data from the European Centre for Medium-Range Weather Forecasts and location data from the OpenStreetMap project. Using weather data for the period 1991 to 2021 it provides an updated Köppen-Geiger climate for geographical points such as towns or cities, as well as for larger areas such as regions or country administration subdivisions. The website has been used as a data source in published research such as the study on ungulate dental ecometrics (Saarinen et al., 2021) indicated in Table 11 or other areas such as evaporative cooling by major climate zones in India (Chopra et al., 2022).

Each population, with the description reproduced from Howells, 1989 is listed in Table 13, along with the location defined on the basis of the information provided. For 10 of the 28 populations, a geographical region was established instead of a specific location. There are various reasons for this: for example, the series of skull used for populations such as the South Africa Zulu or the North Japan Hokkaido were obtained principally from 20th century dissecting rooms, with no indication of locality in the text. Other series are extracted from different points on an island such as the populations of "Tasmania General" or a series of islands such as the "Polynesia Moriori, Chatham Islands", or "Philippine Islands General". In these cases, the different climates for the island (Tasmania), the whole archipelago (Chatham Islands) or the whole country (Philippines) are shown.

Description of population	Males	Females	Location	Climate
Northern Europe: Medieval Norse, Oslo	55	55	Oslo	Dfb
Central Europe: Zalavar, Hungary	53	45	Zalavar	Cfa
Central Europe: Berg, Carinthia, Austria	56	53	Techendorf	Dfb
East Africa: Teita, Kenya	33	50	Voi	BSh
West Africa: Dogon, Mali	47	52	Mopti region	BSh, BWh
South Africa: Zulu	55	46	Kwazulu-Natal region	Cfa, Cfb,BSh, Aw
Australia: Lake Alexandrina Tribes, S. Australia	52	49	Murray Bridge	BSk
Tasmania: General	45	42	Tasmania island	Cfb, Csb
Melanesia: Tolai, New Britain	56	54	East New Britain province	Af
Polynesia: Mokapu, Oahu, Hawaii	51	49	Oahu island	Aw
Polynesia: Easter Island	49	37	Easter Island	As
Polynesia: Moriori, Chatham Islands	57	51	Chatham Islands	Cfb, Csb
North America: Early Arikara	42	27	Pierre, South Dakota	Dfa
North America: Santa Cruz Island, California	51	51	Santa Barbera, California	Csa
South America: Yauyos, Peru	55	55	Chincha Alta, Ica	BWh
North Japan: Hokkaido	55	32	Hokkaido Island	Dfb, Dfa
South Japan: North Kyushu	50	41	Fukuoka prefecture	Cfa
Chinese: Haikou City, Hainan	45	38	Haikou	Cwb
Taiwan Aboriginals: Atayal	29	18	Yilan City	Cfa
Philippine Islands: General	50		Philippine country	Af, Am, Aw, Cwb, Cfb
Guam: Latte Period	30	27	Guam island	Af
Egypt: Gizeh, 26th-30th Dynasties	58	53	Cairo	Bwh
South Africa: Bushman (San)	41	49	Northern Cape	BSh, BSk, BWh, BWk
Andaman Islands: General	35	35	Andaman and Nicobar Islands	Am, Af
Ainu, Japan: South and Southeast Hokkaido	48	38	Hokkaido island	Dfb, Dfa
Sibeira: Buriats	55	54	Baikal	Dwb
Geenland: Inugsuk Eskimo	53	55	Greenland	ET, Dfc
Shang Dynasty Chinese: Anyang	42		Anyang	Cfa
Total	1348	1156		

Table 13. *The 28 populations with their respective climate classification. The description of each population is that used in Howells, 1989.*

Figure 19. *Map of Southern Africa modified from Schuster et al., 2010. The distribution of the Khoisan language, spoken by the San, is indicated by broken red line. The desert area (beige colour) and arid area (green) do not entirely match the Köppen-Geiger classification*

For the population described as West Africa Dogon, Mail, the skulls were described as deriving from burial caves in the Bandiagara plateau, east of the Niger river, in the vicinity of 14°30'N, 30°30'W (Howells, 1989 page 93). However, there must be a typing error in the coordinates as the 30th meridian west lies in the Atlantic Ocean. The Bandiagara plateau is located within the Mopti administrative region of Mali, and this is the location indicated in Table 13 for this population.

In the case of the South Africa Bushman (San), the 90 skulls measured for this series came from the collections of 8 different institutions and giving them a specific location source is problematic. 35 of the skulls, from the Anthropological Institute of Vienna, are described as originating "mostly from various parts of the Kalahari". Of the 30 skulls measured at the South African Museum, Cape Town, 16 had their origin from a cemetery in Colesberg, Northern Cape Province (Howells, 1989 page 111). The specific originating location of the remaining Bushman skulls is not available.

As can be seen from the map of the area where their language is spoken, Figure 19 (Schuster et al., 2010), the 3 largest population regions covered by the Bushman are Botswana (climates BSh, BWh), Namibia (BSh, BWh, BWk) and the Northern Cape (BSh, BSk, BWh, BWk). As the climate classes indicated for the Northern Cape include those for Botswana and Namibia, this is the location shown in Table 13 for the South Africa Bushman (San).

3.8 Choice of reference populations based upon climate

Six of the 28 Howells populations have their origin in an area with one of the Köppen-Geiger climate classifications Csa, BSh or BSk. As can be seen from the summary of these populations in Table 14, four of these six populations are from Africa, one is from North America and one is from Australia.

The Dmanisi skulls will be analysed by bootstrapping with three different reference samples drawn from these six populations. The first reference sample will be made up of the same populations used in the analysis by Rightmire et al., 2019 and composed of the 3 Africa groups Teita, Dogon and Zulu. A second reference sample will be a single population chosen from Table 14. The third and final reference sample based upon ecological choices will be made up of all the six populations in Table 14.

Description of population	Males	Females	Location	Climate
East Africa: Teita, Kenya	33	50	Voi	BSh
West Africa: Dogon, Mali	47	52	Mopti region	BSh, BWh
South Africa: Zulu	55	46	Kwazulu-Natal region	Cfa, Cfb,BSh, Aw
Australia: Lake Alexandrina Tribes, S. Australia	52	49	Murray Bridge	BSk
North America: Santa Cruz Island, California	51	51	Santa Barbera, California	Csa
South Africa: Bushman (San)	41	49	Northern Cape	BSh, BSk, BWh, BWk
Total	279	297		

Table 14. *The six populations with one of the climate areas Csa, BSh or BSk.*

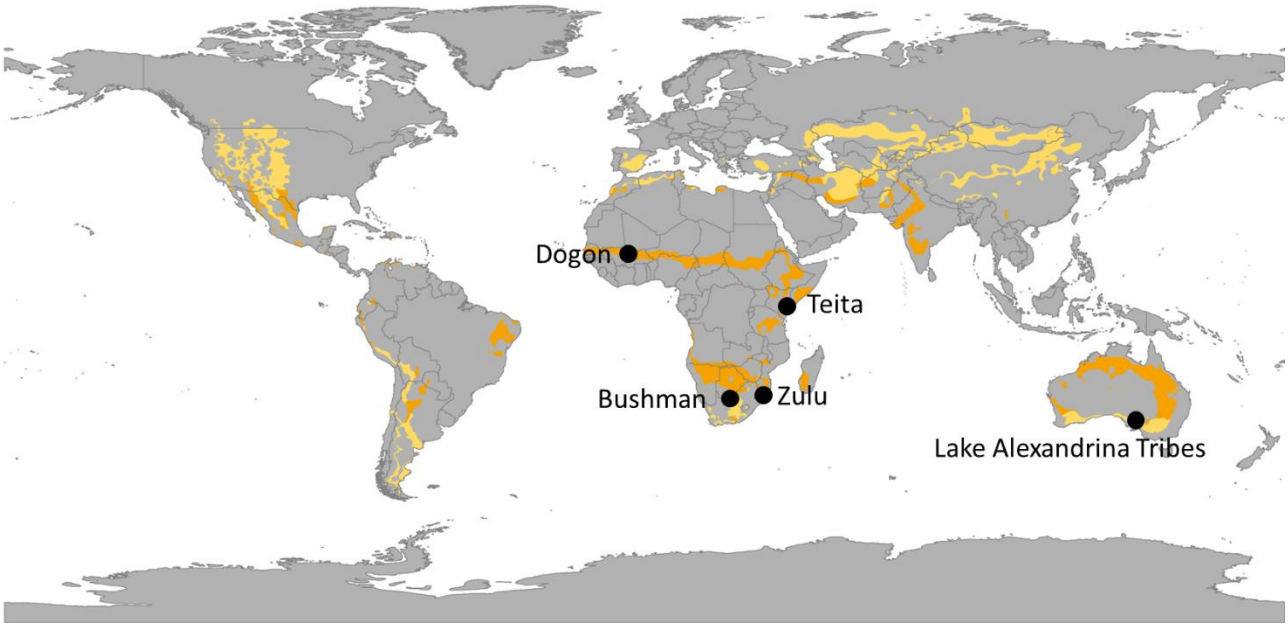

Figure 20. *The five populations of Table 14 located in climate arid steppe zones BSh (shown in orange) or BSk (yellow). Modified from Wikimedia Commons.*

In deciding which single population to use as a reference sample for comparison with the Dmanisi hominins, the description of the composition and source of each series of skulls of Appendix A of Howells, 1989 is pertinent. In particular, the observations in relation to the Lake Alexandrina Tribes of South Australia indicate a well-defined local population, with linguistics and archaeology pointing to a long term stability of perhaps 2000 years. The author goes on to consider that this time-limited and local population could be considered one of the near ideal samples in his 1989 investigation. When the location of this population on the shores of Lake Alexandrina is considered, all the conditions set out for the ideal sample population on an ecological basis are fulfilled:

1.the Lake Alexandrina Tribes represent a single localised population from a relatively short time frame (restricted geographic and time conditions)

2. it includes 52 males and 49 females (morphological condition);

3. it is located in an area with a comparable steppe environment with the presence of a permanent aquatic body (ecological condition).

The maps in Figures 20 and 21 show the populations of Table 14 In their respective climate zones.

Figure 21. *The only population from Table 14 located in the climate zone Csa (shown in bright yellow). Modified from Wikimedia Commons.*

3.9 Results of bootstrapping reference populations chosen on climate basis

For each of the ten measurements, 5000 samples were created from the Howells reference populations by resampling with replacement, with the sample size numbering 4 or 5 to match the number of Dmanisi crania that contributed to a given measurement. The number of samples that produced a measurement CV value exceeding that calculated for the Dmanisi crania was counted, and this number was then divided by 5000 to obtain the percentage value indicated in the tables that follow.

3.10 Bootstrap of 3 Africa group: Teita, Dogon and Zulu

The first bootstrap performed is summarised in Table 15 and uses the three African groups that Rightmire et al., 2019 used in their analysis and which have in common the climate classification BSh.

Measurement	Abb	Dmanisi		3 Africa group		Sample CV > Dmanisi CV	
		n	CV	n	CV	n	%
Glabella-opisthocranion	GOL	4	**5,6**	283	**4,3**	787	**15,7**
Porion-vertex height	VRR	4	**9,6**	283	**4,0**	0	**0,0**
Max cranial breadth	XCB	4	**3,5**	283	**4,4**	2963	**59,3**
Biauricular breadth	AUB	4	**5,2**	283	**3,8**	586	**11,7**
Biasterionic breadth	ASB	5	**4,9**	283	**4,4**	1479	**29,6**
Biorbital chord	FMB	4	**5,2**	283	**4,3**	1042	**20,8**
Bimaxillary chord	ZMB	4	**8,7**	283	**5,5**	219	**4,4**
Cheek height	WMH	4	**8,4**	283	**11,0**	2937	**58,7**
Max. malar height	XML	4	**6,4**	283	**7,2**	2416	**48,3**
Nasal breadth	NLB	4	**6,1**	283	**6,6**	2396	**47,9**

Table 15. *Result of the bootstrap of 3 Africa group. The numbers highlighted in blue show the number and percentage of times the measurement CV of one of the 5000 samples exceed that calculated for the Dmanisi hominins.*

To better understand the data in Table 15, Figure 22 is a graphical representation of the measurement CV's for the Dmanisi and the Africa sample group, with the percentage of times the calculated sample CV of a measurement is greater than that for the fossils indicated in a box.

The extreme variability in cranial height at Dmanisi is confirmed by both the value for the VRR coefficient of variance (9,6 for Dmanisi vs. 4,0 in the case of the 3 Africa reference population) and also by the fact that the bootstrapping performed on the 283 African porion-vertex measurements did not produce one single sample with a CV in excess of 9,6.

Three further Dmanisi braincase measurements GOL, AUB and ASB have CV's in excess of those of the 3 Africa reference population, but the bootstrap procedure confirmed that 15,7%, 11,7% and 29,6% respectively of the samples generated provided higher coefficients of variance. In the case of maximum cranial breadth XCB, the Africa reference group has a higher CV of 4,4 versus 3,5 for the fossils.

The three facial measurements of cheek height, maximum malar height and nasal breadth all show more variability in the 3 Africa reference group. In the case of the biorbital and bimaxillary chords, the Dmanisi fossils show more variability. The bimaxillary chord is particularly variable when

compared to this African reference population, where only 4,4% of the generated samples returned a coefficient of variance in excess of the Dmanisi value.

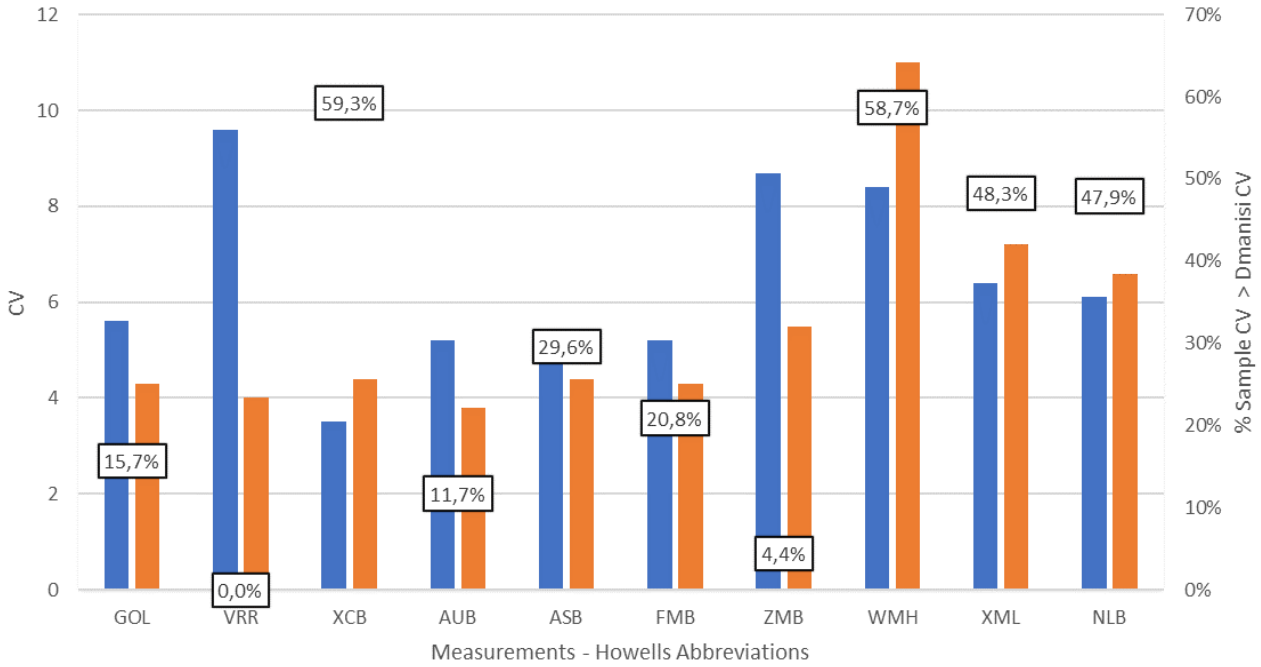

Figure 22. *Dmanisi CV (blue - left axis) compared to Africa CV (red) with % of bootstrap samples exceeding fossil CV indicated in boxes (right axis).*

3.11 Bootstrap of Australia group: Lake Alexandrina Tribes

As discussed earlier, the Lake Alexandrina population is perhaps the most ideal of the reference samples chosen on ecological grounds, representing a time and location restricted population living close to a permanent water body in a comparable steppe ecology to the Dmanisi hominins. The bootstrap technique was applied in the same manner as for the 3 Africa reference population, and the results are summarised in Table 16 in data form and graphically in Figure 23.

Measurement	Abb	Dmanisi		Australia group		Sample CV > Dmanisi CV	
		n	CV	n	CV	n	%
Glabella-opisthocranion	GOL	4	**5,6**	101	**4,0**	543	**10,9**
Porion-vertex height	VRR	4	**9,6**	101	**3,9**	0	**0,0**
Max cranial breadth	XCB	4	**3,5**	101	**4,2**	2439	**48,8**
Biauricular breadth	AUB	4	**5,2**	101	**4,7**	1485	**29,7**
Biasterionic breadth	ASB	5	**4,9**	101	**5,0**	1999	**40,0**
Biorbital chord	FMB	4	**5,2**	101	**4,3**	1023	**20,5**
Bimaxillary chord	ZMB	4	**8,7**	101	**5,8**	321	**6,4**
Cheek height	WMH	4	**8,4**	101	**11,3**	3199	**64,0**
Max. malar height	XML	4	**6,4**	101	**7,5**	2764	**55,3**
Nasal breadth	NLB	4	**6,1**	101	**6,6**	2323	**46,4**

Table 16. *Result of the bootstrap of the single Australia group.*

Once again, the extreme variability in cranial height at Dmanisi is confirmed with the Australia group presenting a CV of just 3,9 for the VRR measurement versus the 9,6 CV value for the Dmanisi hominins. Additionally bootstrapping performed on the 101 Australian porion-vertex measurements

did not produce one single sample with a CV in excess of 9,6. For the other braincase measurements, the Australia group also presents lower CV's for the GOL and AUB measurements compared to Dmanisi and a higher CV for maximum cranial breadth. In the case of biasterionic breadth – ASB – the Australia sample presents slightly more variability with a CV of 5,0 versus 4,9 for the fossils or 4,4 for the 3 Africa group. The bootstrap procedure applied to these four braincase measurements returned CV values higher than the Dmanisi values in a range of 10,9% of samples generated for GOL up to 48,8% of the samples generated for XCB.

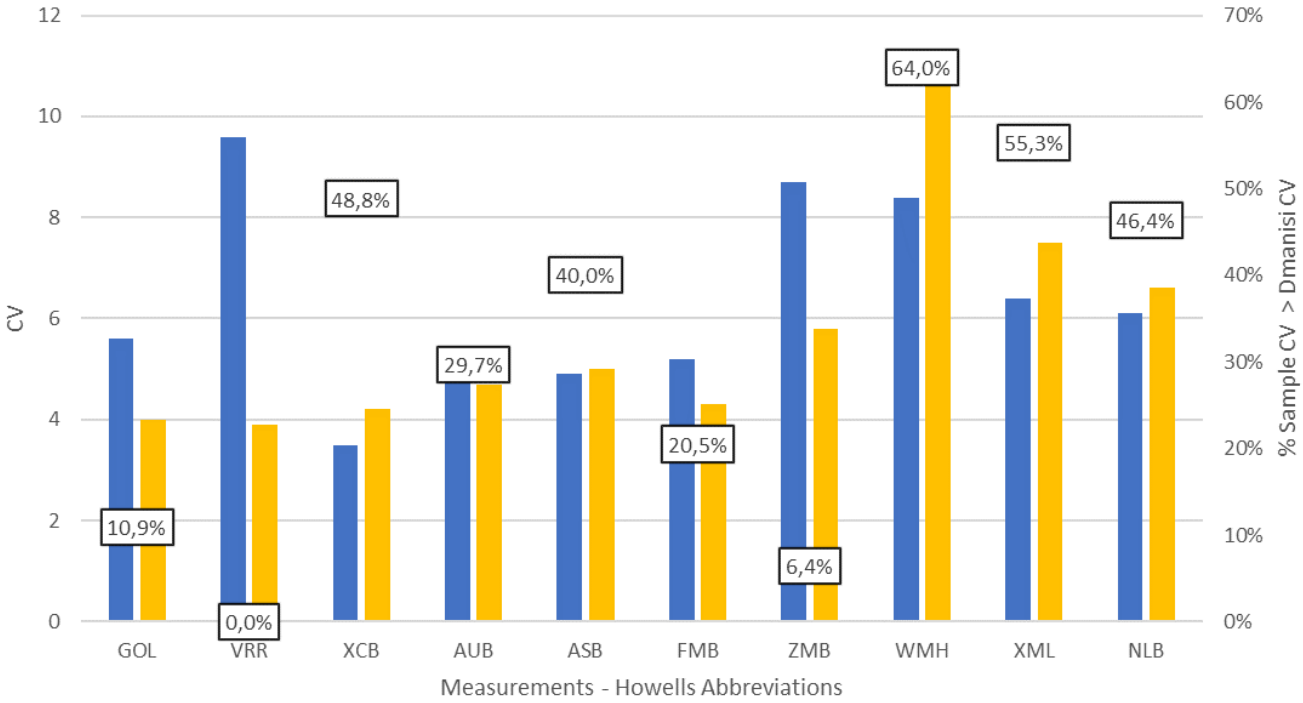

Figure 23. *Dmanisi CV (blue - left axis) compared to Australia CV (yellow) with % of bootstrap samples exceeding fossil CV´s indicated in boxes (right axis).*

The variability in facial dimensions of the Australia population when compared to the Dmanisi group presents a similar picture to that of the African group. The three facial dimensions of cheek height, maximum malar height and nasal breadth all show more variability in the Australia and Africa reference groups. In the case of the biorbital and bimaxillary chords, the Dmanisi fossils show more variability then both the Australia and Africa groups. Once more the bimaxillary chord – measurement ZMB - is particularly variable when compared to the Australia reference population, where only 6,4% of the bootstrap generated samples returned a coefficient of variance in excess of the Dmanisi value.

3.12 Bootstrap of World group

The final reference population based upon climatic considerations is made up of all the populations listed in Table 14. The 3 Africa populations used in Section 3.10 will be combined with the Australia population used in the analysis in Section 3.11. To this combined group we will add the Santa Cruz Island population from California, North America - the only population measured by Howells that is found in the Csa climate zone - and the Bushman group from South Africa. This "World" reference population made up of 576 individuals, contains the three climate areas defined in Table 12. Its CV's and bootstrap results are summarised in Table 17 and graphically in Figure 24.

Measurement	Abb	Dmanisi		World group		Sample CV > Dmanisi CV	
		n	CV	n	CV	n	%
Glabella-opisthocranion	GOL	4	**5,6**	576	**4,5**	1005	**20,1**
Porion-vertex height	VRR	4	**9,6**	576	**4,7**	17	**0,3**
Max cranial breadth	XCB	4	**3,5**	576	**4,5**	2997	**59,9**
Biauricular breadth	AUB	4	**5,2**	576	**5,5**	2089	**41,8**
Biasterionic breadth	ASB	5	**4,9**	576	**5,2**	2301	**46,0**
Biorbital chord	FMB	4	**5,2**	576	**4,5**	1348	**27,0**
Bimaxillary chord	ZMB	4	**8,7**	576	**5,8**	416	**8,3**
Cheek height	WMH	4	**8,4**	576	**11,5**	3109	**62,2**
Max. malar height	XML	4	**6,4**	576	**8,0**	2799	**56,0**
Nasal breadth	NLB	4	**6,1**	576	**8,6**	3380	**67,6**

Table 17. *Result of the bootstrap of the World reference group.*

This larger combined World reference group, with populations extracted from three continents, yields higher coefficients of variance for all ten measurements than the other two groups which were restricted to single continents. Despite this, the Dmanisi fossils show greater variability in cranial length – GOL – and cranial height – VRR. Indeed, the bootstrapping performed on the 576 porion-vertex measurements of this combined group produced just 17 samples, equivalent to 0,3%, with a CV in excess of 9,6. With regards the other three braincase measurements, XCB, AUB and ASB, the world group presents higher variability in all of these, whereas the Australia group showed higher variability for just biasterionic breadth – ASB or the Africa group only showing higher variability for maximum cranial breadth – XCB.

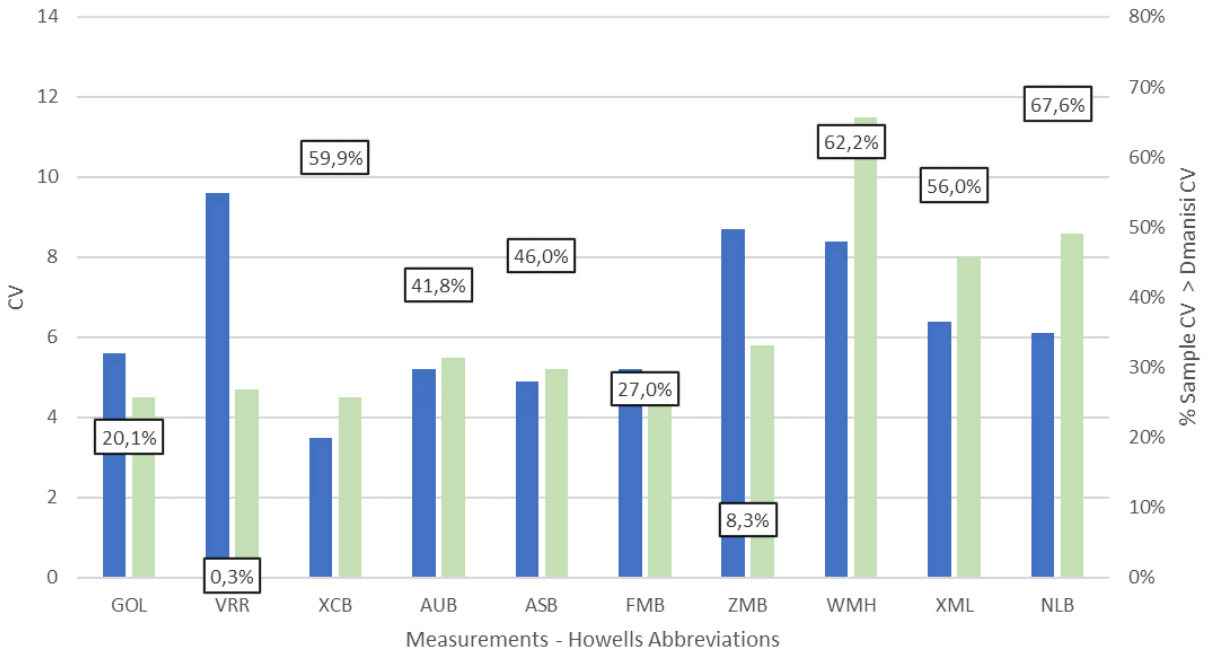

Figure 24. *Dmanisi CV (blue - left axis) compared to World CV (green) with % of bootstrap samples exceeding fossil CV indicated in boxes (right axis)*

The analysis of variability in facial dimensions of the World population versus the Dmanisi group presents the same conclusions as seen in the prior two groups. The three facial dimensions of cheek height, maximum malar height and nasal breadth all show more variability in the World, Australia and 3 Africa reference groups. In the case of the biorbital and bimaxillary chords, the Dmanisi fossils show more variability then do any of the three reference populations. Once more the bimaxillary chord – measurement ZMB – with a coefficient of variance of 8,7 at Dmanisi compared with 5,8 for the World group, shows high variability. Just 8,3% of the samples generated from the World group returned a coefficient of variance in excess of the equivalent Dmanisi statistic.

3.13 Preparation of extreme reference population

The pensize statistic was formulated in Howells, 1973 and 1989 to indicate relative cranial size across the different population groups analysed. Using separate male and female mean of means and the standard deviation of pooled within-group variances for each of the 57 Howells measurements, the Z-score is calculated for each individual measurement of each individual cranium as follows:

Z-score = (measurement – mean of means) x 10 / (pooled within group standard deviation)

The pensize for each cranium is then defined as:

$$PENSIZE = (Z_1 + Z_2 + \ldots + Z_{57}) / 57$$

where Z_1 to Z_{57} are the Z scores for each of the 57 measurements. The average pensize is then calculated for each series of male and female crania for each population. Table 18 summarises the pensize data extracted from Howells, 1989. A weighted pensize statistic was then calculated for this study based upon the number of males and females in each population. Populations with generally larger crania show a higher positive pensize, whereas populations with generally smaller skulls have a lower and negative pensize.

3.14 Choice of extreme reference populations

Two extreme reference samples will be formulated for subsequent bootstrap analysis of the Dmanisi fossils. The first reference sample will be composed of the two populations at the end of either extreme, the small-skulled Andaman Islanders (weighted pensize of -11,70) and the large-skulled Siberian Buriats (weighted pensize of 5,74). These populations are highlighted in grey in Table 18.

The second reference sample will be geographically limited and extracted from two of the four African groups listed in Table 14. The lower extreme of this reference sample will be composed of the South African San which have the second smallest pensize after the Andaman Islanders with a value of -9,48. The Zulu group with a pensize of 0,14 has the highest value for this statistic when compared with the Teita (-1,53) or the Dogon (-4,75). This second reference sample is highlighted in yellow in Table 18.

Population	Pensize		Number		Weighted
	Male	Female	Males	Females	Pensize
Northern Europe: Medieval Norse, Oslo	0,70	1,21	55	55	0,96
Central Europe: Zalavar, Hungary	-0,30	-0,01	53	45	-0,17
Central Europe: Berg, Carinthia, Austria	-0,40	-0,53	56	53	-0,46
East Africa: Teita, Kenya	-1,64	-1,46	33	50	-1,53
West Africa: Dogon, Mali	-5,47	-4,10	47	52	-4,75
South Africa: Zulu	-1,13	1,66	55	46	0,14
Australia: Lake Alexandrina Tribes, S. Australia	1,41	0,99	52	49	1,21
Tasmania: General	-0,19	-0,45	45	42	-0,32
Melanesia: Tolai, New Britain	0,72	0,86	56	54	0,79
Polynesia: Mokapu, Oahu, Hawaii	5,15	3,58	51	49	4,38
Polynesia: Easter Island	6,78	4,26	49	37	5,70
Polynesia: Moriori, Chatham Islands	4,47	4,96	57	51	4,70
North America: Early Arikara	1,43	1,42	42	27	1,43
North America: Santa Cruz Island, California	-1,75	-2,17	51	51	-1,96
South America: Yauyos, Peru	-5,58	-6,02	55	55	-5,80
North Japan: Hokkaido	-0,08	-2,02	55	32	-0,79
South Japan: North Kyushu	-1,24	-1,66	50	41	-1,43
Chinese: Haikou City, Hainan	-2,84	-0,51	45	38	-1,77
Taiwan Aboriginals: Atayal	-6,19	-5,09	29	18	-5,77
Philippine Islands: General	-2,63		50		-2,63
Guam: Latte Period	5,44	5,05	30	27	5,26
Egypt: Gizeh, 26th-30th Dynasties	-2,55	-2,82	58	53	-2,68
South Africa: Bushman (San)	-10,48	-8,64	41	49	-9,48
Andaman Islands: General	-12,28	-11,12	35	35	-11,70
Ainu, Japan: South and Southeast Hokkaido	3,90	2,85	48	38	3,44
Sibeira: Buriats	5,88	5,60	55	54	5,74
Geenland: Inugsuk Eskimo	3,91	4,68	53	55	4,30
Shang Dynasty Chinese: Anyang	-0,16		42		-0,16

Table 18. *Weighted pensize statistic calculated from male and female pensize data extracted from Table 3 in Howells, 1989. Highlighted in grey the Extreme World population group. Highlighted in yellow, the Extreme Africa population group.*

3.15 Results of bootstrapping extreme reference populations

The composition of the two extreme reference population groups is represented on the map in Figure 25. The same bootstrap procedure described in section 3.9 will be performed, and the percentage value for the number of samples that produce a measurement CV value exceeding that calculated for the Dmanisi crania will be determined.

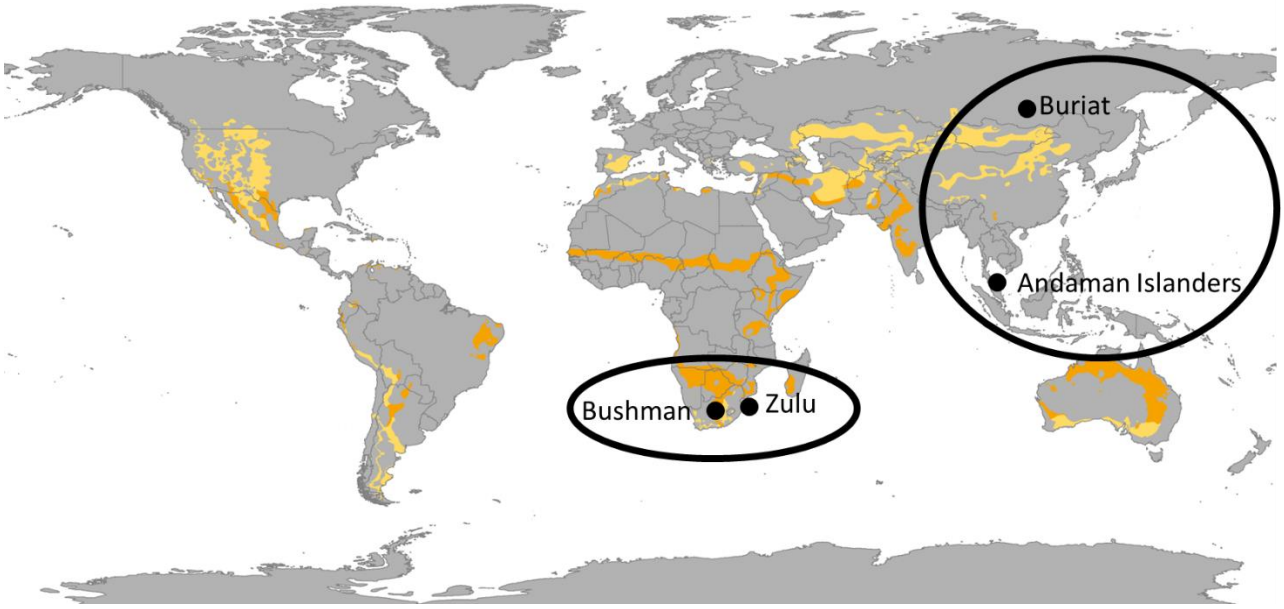

Figure 25. *Map showing composition and location of the two extreme reference group, placed on the map of BSk and BSh climate zones. Modified from Wikimedia Commons.*

3.16 Bootstrap of Extreme World population

The coefficients of variance and the data for the bootstrap of this extreme group composed of Siberian Buriats and Andaman Islanders can be found in Table 19 and is represented graphically in Figure 26.

Measurement	Abb	Dmanisi		Extreme World group		Sample CV > Dmanisi CV	
		n	CV	n	CV	n	%
Glabella-opisthocranion	GOL	4	**5,6**	179	**5,5**	2018	**40,4**
Porion-vertex height	VRR	4	**9,6**	179	**4,0**	0	**0,0**
Max cranial breadth	XCB	4	**3,5**	179	**7,5**	4518	**90,4**
Biauricular breadth	AUB	4	**5,2**	179	**9,8**	4351	**87,0**
Biasterionic breadth	ASB	5	**4,9**	179	**8,9**	4565	**91,3**
Biorbital chord	FMB	4	**5,2**	179	**6,0**	2600	**52,0**
Bimaxillary chord	ZMB	4	**8,7**	179	**7,2**	1075	**21,5**
Cheek height	WMH	4	**8,4**	179	**19,3**	4561	**91,2**
Max. malar height	XML	4	**6,4**	179	**9,2**	3604	**72,1**
Nasal breadth	NLB	4	**6,1**	179	**9,5**	3817	**76,3**

Table 19. *Bootstrap result of the Extreme World group of Andaman Islanders and Siberian Buriats*

This Extreme World group yields higher coefficients of variance compared to the Dmanisi fossils for three of the five braincase measurements and for four of the five facial measurements. Cranial length - GOL - is marginally more variable at Dmanisi, yielding a CV of 5,6 compared to a value of 5,5 for the Extreme World group. However, once again, the high variability in the Dmanisi cranial height is evident when compared with this reference sample. The CV for porion-vertex height of the Extreme World group is 4,0 and the bootstrapping performed on the 179 VRR measurements of this group did not produce any samples with a CV in excess of 9,6.

The bimaxillary chord – ZMB - at Dmanisi is the only facial measurement to show greater variability when compared to the Extreme World group, though 21,5% of the bootstrap samples present a higher CV for this measurement – the highest percentage value for this measurement of all reference samples in this study. Additionally, the pattern seen in prior reference samples of higher variability in *Homo sapiens* for cheek height, maximum malar height and nasal breadth is also reflected in this sample.

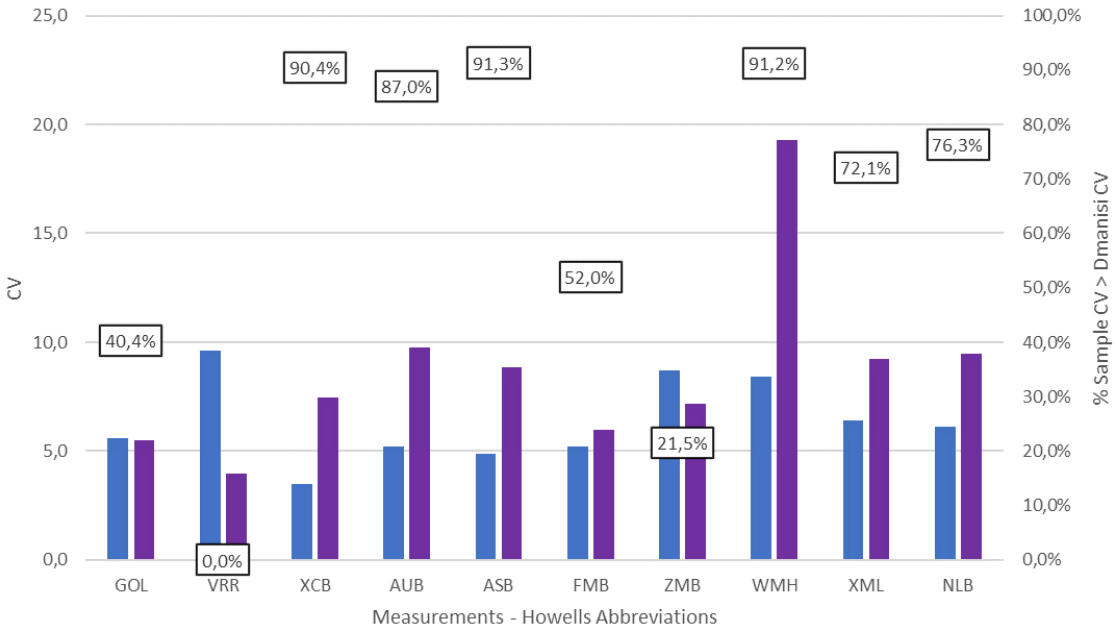

Figure 26. *Dmanisi CV (blue - left axis) compared to Extreme World CV (purple) with % of bootstrap samples exceeding fossil CV indicated in boxes (right axis)*

The high 19,3 coefficient of variance for WMH seen in Figure 26 is explained by the high Siberian Buriat cheeks. The males of that population group have a mean WMH of 28,96 (page 130 Howells, 1989) versus a mean of means for the 18 populations groups of 23,37 as seen in Table 5. The standard deviation on pooled group variances for WMH is 2,22 (page 10 Howells, 1989) meaning that the average male Siberian Buriat cheek heights is (28,96-23,37) / 2,22 = 2,52 standard deviations above the 18 population mean of means. The same calculation for the female Buriats yields a value of 2,59 standard deviations.

The high coefficient of variance in cheek height of this reference sample highlights one of the weaknesses of the extreme reference population selection method. Not only have we chosen two populations from either end of the size range and geographically wide apart, they also come from extremely different climate zones, introducing further variability into the reference population. As seen in Table 13, the Andaman Islanders are located within equatorial climates zones Am and AF. The Siberian Buriats are located in the snow dominated climate zone of Dwb.

3.17 Bootstrap of Extreme Africa population

As can be seen from the map in Figure 25 and the data in Table 14, the two populations that make up this reference sample not only share geographic proximity, but they also share a similar climate, namely BSh – Hot Steppe. The combination of these two factors will give additional weight to any conclusions obtained from the analysis of this reference population with the Dmanisi fossils.

Measurement	Abb	Dmanisi		Extreme Africa group		Sample CV > Dmanisi CV	
		n	CV	n	CV	n	%
Glabella-opisthocranion	GOL	4	**5,6**	191	**4,2**	744	**14,9**
Porion-vertex height	VRR	4	**9,6**	191	**5,8**	130	**2,6**
Max cranial breadth	XCB	4	**3,5**	191	**4,0**	2413	**48,3**
Biauricular breadth	AUB	4	**5,2**	191	**4,6**	1428	**28,6**
Biasterionic breadth	ASB	5	**4,9**	191	**4,7**	1808	**36,2**
Biorbital chord	FMB	4	**5,2**	191	**4,8**	1562	**31,2**
Bimaxillary chord	ZMB	4	**8,7**	191	**5,8**	359	**7,2**
Cheek height	WMH	4	**8,4**	191	**11,2**	3113	**62,3**
Max. malar height	XML	4	**6,4**	191	**8,9**	3350	**67,0**
Nasal breadth	NLB	4	**6,1**	191	**8,2**	3419	**68,4**

Table 20. *Bootstrap result of the Extreme Africa group composed of the Zulu and Bushman groups*

For the five braincase measurements in Table 20, only maximum cranial breadth of the Extreme Africa group reveals a higher coefficient of variance compared to the Dmanisi fossils. The extreme variability in cranial height at Dmanisi is once again confirmed by the respective values for the VRR coefficient of variance (9,6 for Dmanisi vs. 5,8 in the case of the Extreme Africa reference sample) but significantly, 2,6% of the 5000 bootstrap samples performed on the 191 Extreme African porion-vertex measurements produced samples with a CV in excess of that of Dmanisi.

Three further Dmanisi braincase measurements GOL, AUB and ASB show higher variability than those of the Extreme Africa reference sample, but the bootstrap exercise confirmed that 14,9%, 28,6% and 36,2% of the samples generated provided higher coefficients of variance.

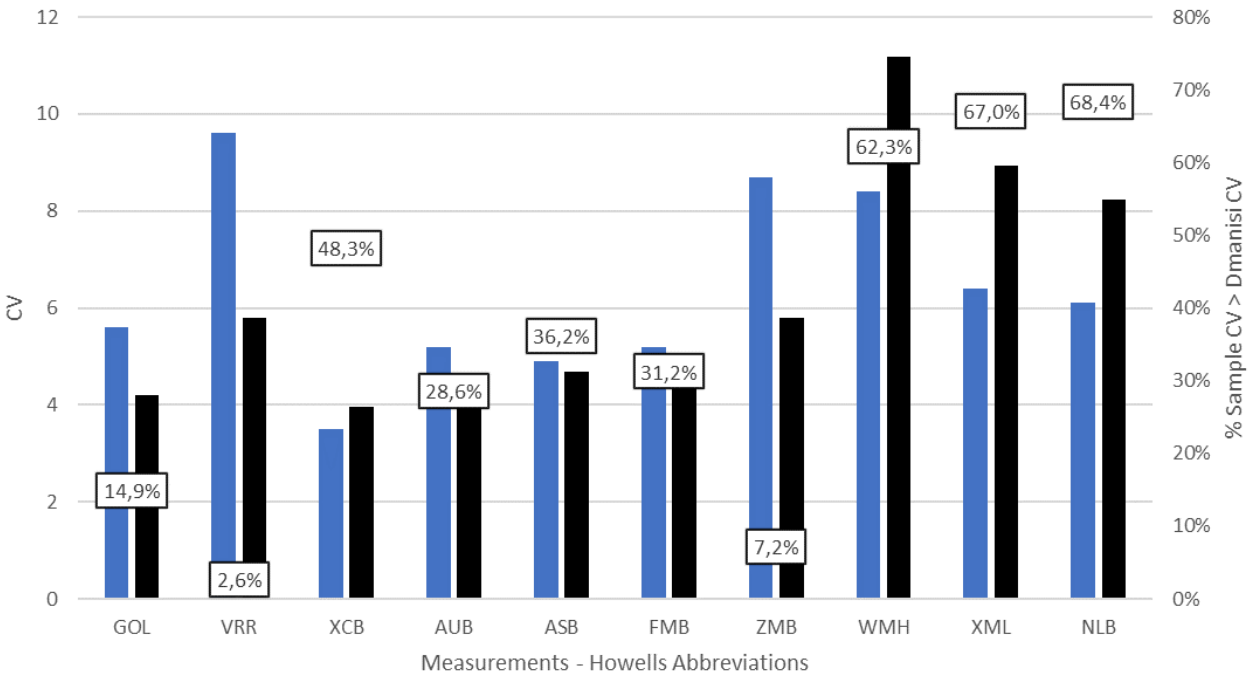

Figure 27. *Dmanisi CV (blue - left axis) compared to Extreme Africa CV (black) with % of bootstrap samples exceeding fossil CV indicated in boxes (right axis)*

As seen in all the other reference samples, the three facial dimensions of cheek height, maximum malar height and nasal breadth all show more variability in the Extreme Africa reference group. The Dmanisi fossils show more variability in the biorbital and bimaxillary chords. The bimaxillary chord is particularly variable when compared to the African reference population, where only 7,2% of the generated samples returned a coefficient of variance in excess of the Dmanisi value.

4. DISCUSSION

The visual representation of the coefficients of variance and bootstrap percentages presented in Figures 22, 23, 24, 26 and 27 have been consolidated into two further visual representations for the purposes of the following discussion. Figure 28 represents the consolidation of the braincase graphic data, and Figure 29 displays that for the facial skeleton. The same colours previously used for individual reference populations are maintained here.

4.1 Braincase measurements

The coefficient of variance for the braincase measurements of the five reference populations compared with the Dmanisi fossils are summarised in graphic form in Figure 28 with an indication of the percentage of bootstrap samples exceeding each fossil coefficient of variance displayed in a box.

In cranial length – abbreviation GOL – the Dmanisi fossils with a CV of 5,6 show greater variability than all the other five reference populations. The Extreme World population – composed of Siberian Buriats and Andaman Islanders - has a marginally smaller CV of 5,5 with 40,4% of the bootstrap samples returning a higher CV than that for the Dmanisi hominins for this measurement. The other reference populations yielded higher CV's ranging from 10,9% of the bootstrap samples for the Australian Lake Alexandrina Tribes to 20,1% of the bootstrap samples for the World reference group composed of all populations falling within the Csa, BSk and BSh climate zones. On the basis of these percentages, we cannot state that the cranial length of the Dmanisi fossils exceeds that of the modern human reference populations.

The CV for Dmanisi cranial height – measurement VRR – is 9,6 and completely overshadows the values for the 3 Africa group (4,0), Australia (3,9), World group (4,7), Extreme World (4,0) and Extreme Africa (5,8). As we have seen in the above results and as summarised in Figure 28, the samples generated by bootstrapping of three of the populations did not produce a single case with a coefficient of variance in excess of the 9,6 CV of the Dmanisi VRR measurement. Only the World group and the Extreme Africa group yielded bootstrap samples with a CV higher than that of Dmanisi: 0,3% and 2,6% respectively. The 2,6% result for the Extreme Africa group is significant and confirms that we cannot consider the variability in cranial height of the Dmanisi fossils as exceeding that of this reference population.

The variability in maximum cranial breath – XCB - at Dmanisi is inferior to that of all the modern human reference populations we have compared it to. The CV for this measurement at Dmanisi is 3,5, and the reference population with the closest value to this is from the Extreme Africa group with a value of 4,0.

For biauricular breadth – AUB - Dmanisi presents a higher coefficient of variance when compared to the 3 Africa group, Australia group and the Africa Extreme group. The Dmanisi CV of 5,2 presents its largest difference with the CV of 3,8 of the 3 Africa group. However, 11,7% of the bootstrap

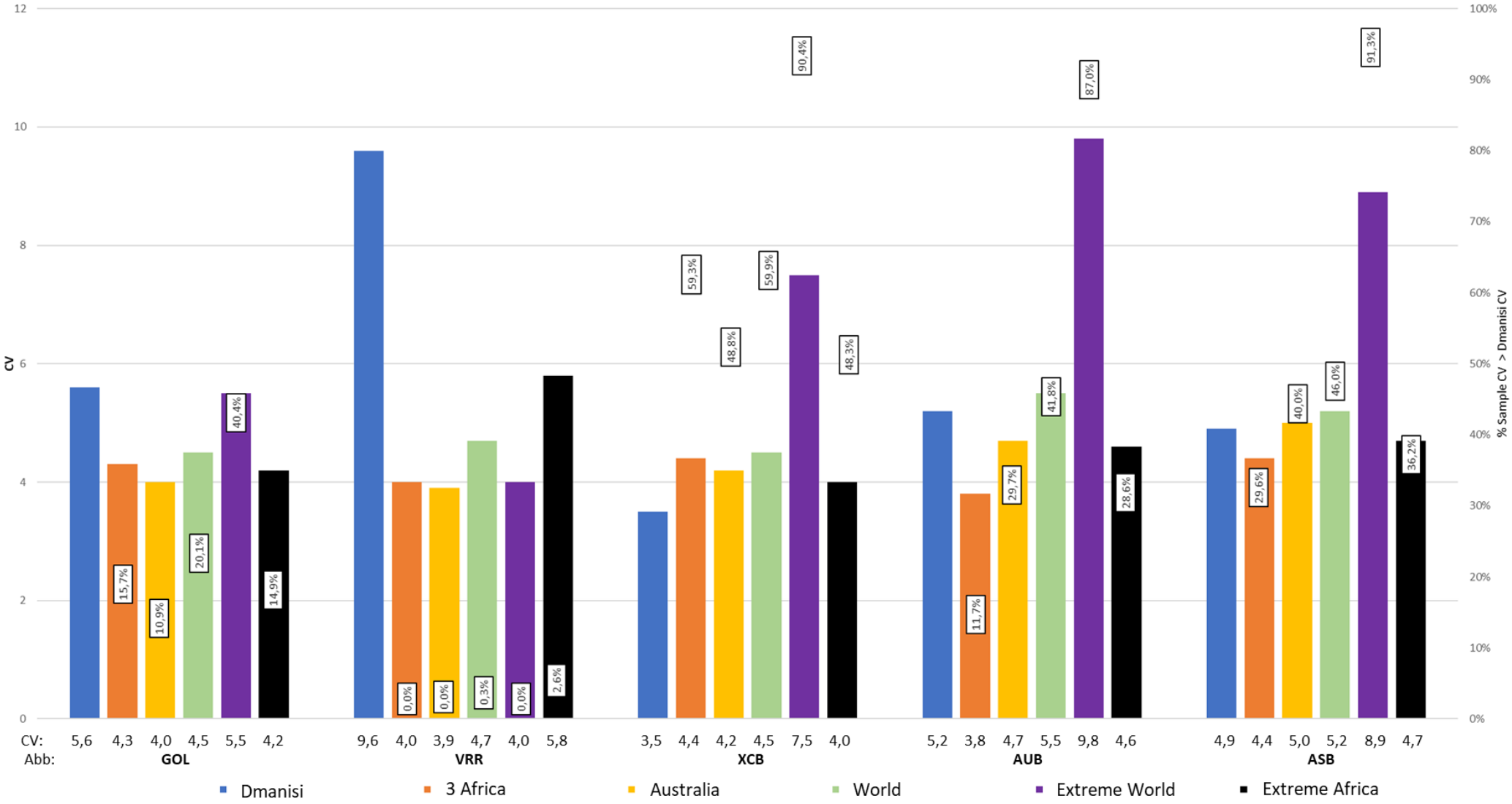

Figure 28. *Dmanisi coefficient of variances (left axis) of braincase measurements compared with those of reference populations included in this study with % of bootstrap samples exceeding Dmanisi CV indicated in boxes (right axis)*

generated samples from the 3 Africa group returned a coefficient of variance in excess of the Dmanisi value. With this percentage value, we cannot conclude that there is more variability in the AUB measurement at Dmanisi when compared with the Africa group composed of the Teita, Dogon and Zulu populations.

The coefficient of variance of 4,9 for biasterionic breadth – ASB – at Dmanisi only exceeds that of the 3 Africa population (4,4) and the Extreme Africa population (4,7). The bootstrap generated samples of these two groups however returned greater coefficients of variance from 29,6% and 36,2% of their respective samples.

4.2 Facial measurements

The coefficient of variance of the facial measurements for each of the five reference populations compared with the Dmanisi fossils is summarised in graphic form in Figure 29 with an indication of the percentage of bootstrap samples exceeding each fossil coefficient of variance displayed in a box.

At Dmanisi the biorbital chord – measurement FMB – with a CV of 5,2 shows more variability when compared with four of the five reference populations. The bootstrap samples of those 4 reference populations yielded a higher CV in 20,5% to 31,2% of cases. Only the Extreme World group shows more variability with a CV of 6,0.

The variability in the bimaxillary chord – ZMB – is clearly greater in the Dmanisi fossils than in all the modern human reference populations we have examined. The bootstrap generated samples of the reference populations reflect this high degree of variability, returning a coefficient of variance in excess of the Dmanisi value in less than 10% of the extracted samples for the 3 Africa, Australia, World and Extreme Africa groups, with only the Extreme World reference population yielding a higher value at 21,5%.

The WMH or cheek height measurement at Dmanisi with a coefficient of variance of 8,4 shows less variability when compared with all the other reference populations of this study, which yield CV's between 11,0 and 11,5 for the 3 Africa, Australia, World and Extreme Africa groups, and the exceptionally high 19,3 for the World Extreme reference population whose high variability was discussed in Section 3.16 above. This is the only cranial measurement of the ten in this study where more than 50% of all the bootstrap samples of all the reference populations yielded a higher CV than the Dmanisi CV.

A further facial measurement with less variability among the Dmanisi hominis compared to the modern human reference populations used in this study is XML or maximum malar height. The Dmanisi coefficient of variance of 6,4 for this measurement compares to a range falling between 7,2 for the 3 Africa population group and 9,2 for the Extreme World group.

The final facial measurement in this study – nasal breadth, with abbreviation NLB – also shows more variability in the five reference populations than in the Dmanisi hominins: the CV's for the five modern population groups range from 6,6 to 9,5 whereas the Dmanisi fossils have a coefficient of variance of 6,1.

4.3 Patterns of variability

The Dmanisi fossils display more variability than all the modern human groups in three measurements: cranial length (GOL), cranial height (VRR) and bimaxillary breadth (ZMB). Arguably,

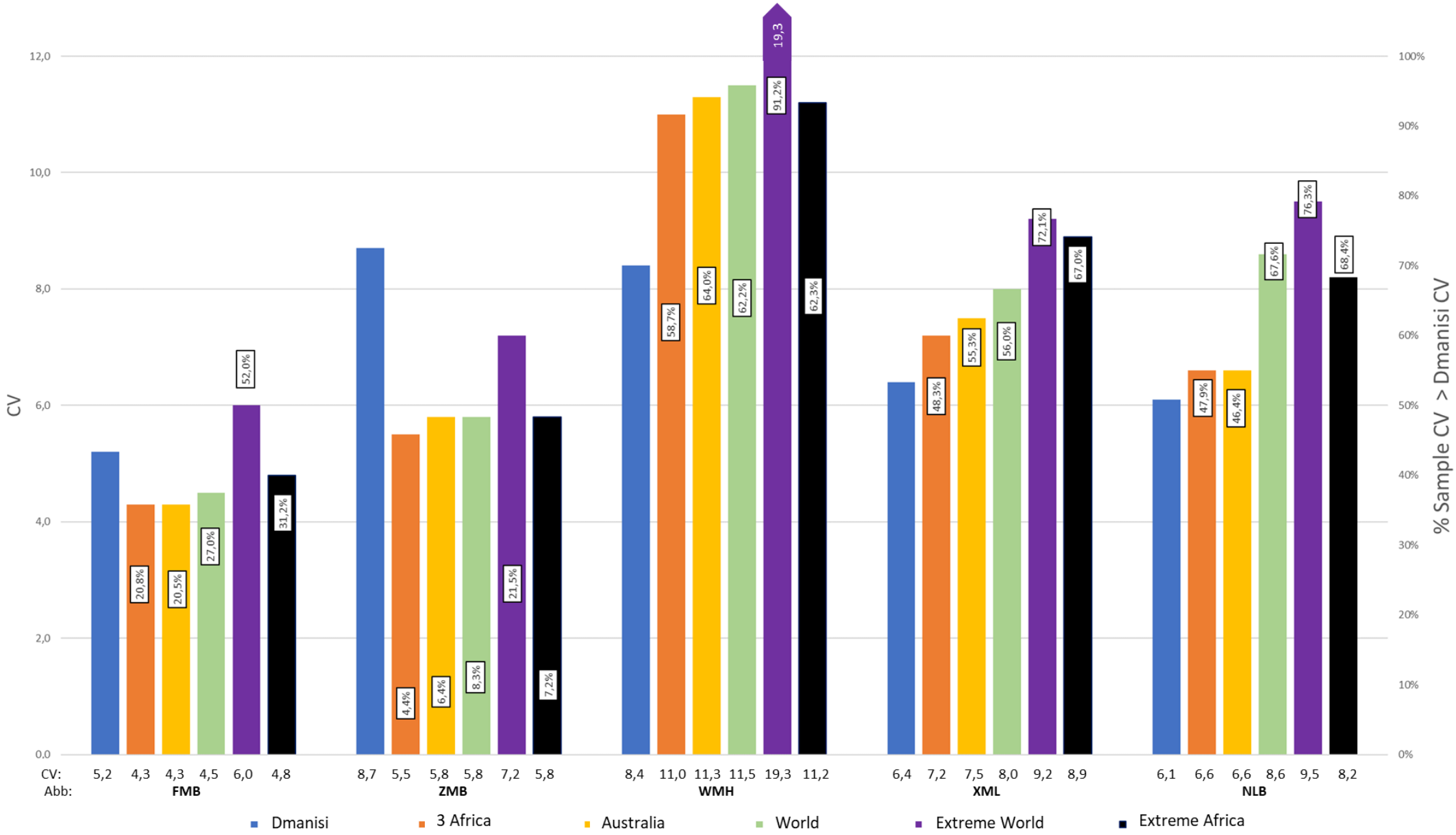

Figure 29. *Dmanisi coefficient of variances (left axis) for facial measurements compared with those of reference populations included in this study with % of bootstrap samples exceeding Dmanisi CV indicated in boxes (right axis). The left axis is limited to a CV value of 12,0, cutting off the CV value for cheek height – WMH - of 19,3 for the Extreme World population.*

biorbital breadth (FMB) could be included in this list as the only human group that showed greater variability in this measurement was the Extreme World group of Siberian Buriats and Andaman Islanders.

All modern human reference populations in this study show greater variability than the Dmanisi fossils in maximum cranial breadth (XCB), cheek height (WMH), maximum malar height (XML) and nasal breadth (NLB). In the case of biauricular breadth (AUB) and biasterionic breadth (ASB), the comparison of variability between the fossils and modern human groups is less conclusive. For AUB two of the five human groups showed a great variability compared to the Dmanisi hominins, and in the case of ASB three of the five human groups showed greater variability.

The Dmanisi hominins show a suite of variability characteristics in three of the analysed measurements and this contrasts with that shown by the modern human groups included in this study which show variability in a different set of four measurements. Different patterns of variability in the fossil and modern human groups are therefore apparent from this analysis.

5 CONCLUSION

In concluding about the number of species present in Dmanisi based upon the above analysis of selected cranial measurements, it is worthwhile considering whether other factors beyond morphological considerations might prompt our search for evidence of multiple taxa at Dmanisi, and to ask whether it might be reasonable to expect to discover more than one species at this site.

5.1 Is it reasonable to expect more than one species at Dmanisi?

Looking at the African continent 300 kya (thousand years ago) there is evidence for the presence of several human species. Modern humans were present at Jebel Irhoud in Northern Africa approximately 315 kya, contemporaneous with both *Homo naledi* in Southern Africa and *Homo heidelbergensis* in Central Africa. There is additionally genetic evidence in sub-Saharan Africans of at least one further archaic ghost lineage (Galway-Witham et al., 2019). In spite of covering a vast continent with inevitable ecological barriers, such a diversity of species raises the possibility of the use over time of the same shelters, hunting areas or watering spaces.

Denisova cave in Siberia has yielded hominin fossils from three different species. A Bayesian analysis of the calibrated radiocarbon age of the fossils indicates that Denisovans, Neanderthals and modern humans coincided in the cave within a period of 50,000 years from 150 to 100 kya (Douka et al., 2019). Genetic research has further confirmed the close contact between species at the cave with the sequencing of the genome of an individual with a Neanderthal mother and a Denisovan father (Slon et al., 2018).

The Middle Paleolithic provides proof of a period of 150 kya of contemporaneous occupation of the Levant by both Neanderthals and modern humans. Sites such as Kebara Cave yield evidence of Neanderthal occupation levels dated to between 59,9±3,5 kya to 51,9±3,5 kya, and later modern human occupation levels dated to between 47 kya and 44 kya (Shea, 2003).

The replacement of Neanderthals by modern humans in Western Europe took place within a time span of 10,000 years between 45 kya and 35 kya. The incoming humans left evidence of their Aurignacian lithic tools at sites in southwestern France such as Saint Césaire, Laussel, or Roc-de-Combe where evidence of prior Neanderthal occupation is documented by the presence of Châtelperronian lithic technology (Mellars & French, 2011).

The above evidence from the archaeological record points to a multiplicity of hominin species with the potential for jointly occupying within a short chronology not only wide geographic areas but also specific locations such as caves or rock shelters. The contact between the species can even be so close as to cause interbreeding. It is therefore not unreasonable to raise the hypothesis that the Dmanisi fossil hominins, deposited within a chronology of at most 80 thousand years, might represent two or more taxa.

5.2 The null hypothesis of a single species cannot be rejected

Of the five modern human populations used as references in this study, the Extreme Africa group composed of the Bushman and Zulu tribes of South Africa represents the most robust reference population, considering their geographic proximity and their sharing one of the climate zones identified in Table 12.

This reference population is effectively a synthesis of the selection methods recommended in Plavcan & Cope, 2001, given that it is based upon both ecological and extreme selection criteria. In addition to being composed of two populations lying at measurement extremes, this reference population respects the restricted geographic and time conditions, includes both females and males, and respects the requirement of sharing a comparable climate.

That this reference population is composed of two tribes at opposite ends of the size spectrum should not overshadow the fact that both groups are members of the same species, namely *Homo sapiens*. Additionally, when reviewing in Table 14 the climate zones for the San - BSh and BWh – and for the Zulu - Cfa, Cfb, BSh, and Aw – the fact that they share just one climate zone – BSh – is sufficient for our purposes: it confirms that both tribes are adapted to survive in a similar climate zone. Finally, the BSh zones for both tribes have important aquatic bodies present, similar to Dmanisi 1,8 Mya: the Okavango Delta, Botswana in the case of the San, and the Pongola River, South Africa in the case of the Zulu. The Extreme Africa reference population fully satisfies the conditions listed in Section 3.2 for an ecological reference sample.

As we have seen in the above analysis, at Dmanisi porion vertex height, measurement VRR, commonly referred to as cranial height, shows great variability when compared with all the modern human reference populations we have reviewed. However, in the case of the Extreme Africa population, a significant, 2,6% of the 5000 bootstrap samples returned a coefficient of variance for VRR in excess of that of Dmanisi. On the basis of this number, we cannot reject the null hypothesis.

A similar conclusion can be retained for cranial length (GOL) and bimaxillary breadth (ZMB). In the case of GOL, 14,9% of the 5000 bootstrap samples of the Extreme Africa group returned higher coefficients of variance for that measurement than the coefficient of variance for Dmanisi. In the case of measurement ZMB the percentage was 7,2%. These results do not provide a basis for rejecting the null hypothesis. A review of Table 20 and Figure 27 draws the same conclusion for the other 7 measurements of the Dmanisi hominins when compared to the Extreme Africa group.

For the ten cranial measurements analysed in this thesis, the variability displayed by the Dmanisi crania when compared to modern human populations is not sufficiently great to conclude that there might be more than one taxon present at Dmanisi. The null hypothesis cannot be rejected.

5.3 Patterns of variability in hominin species

It is important to note that cranial measurements do not share a similar variability within a given population. The Dmanisi hominins exhibit coefficients of variance ranging from 3,5 (XCB) to 9,6 (VRR) whereas for the 3 Africa group the range is from 3,8 (AUB) to 11 (WMH - Table 15) or in the case of the Australia group from 3,9 (VRR) to 11,3 (WMH - Table 16).

The fact that a measurement such as cranial height – VRR in Figure 28 – shows great variability at Dmanisi should not necessarily be interpreted as a possible indication of the presence of two species. A further interpretation could be that the Dmanisi hominins did inherently possess more variability in that measurement, precisely in the same way that cheek height – WMH in Figure 29 – is significantly more variable in modern human groups than in the Dmanisi hominins.

Similar comments could be made for the greater variability at Dmanisi of the bimaxillary chord (ZMB in Figure 29) or the greater variability shown by modern humans in the maximum malar height (XML in Figure 29). This data points to different patterns of variability between fossil and modern human groups with each one exhibiting a different (greater or lesser) variability in any given measurement.

6 BIBLIOGRAPHY

Agustí, J., & Lordkipanidze, D. (2011). How " African" was the early human dispersal out of Africa? *Quaternary Science Reviews*, *30*(11–12), 1338–1342. https://doi.org/10.1016/j.quascirev.2010.04.012

Ambers, A., Elwick, K., Cropper, E. R., Brandhagen, M. D., Jones, B., Durst, J., Gilmore, K. K., Bruseth, J. E., & Gill-King, H. (2021). Mitochondrial DNA analysis of the putative skeletal remains of Sieur de Marle: Genetic support for anthropological assessment of biogeographic ancestry. *Forensic Science International*, *320*. https://doi.org/10.1016/j.forsciint.2021.110682

Belmaker, M., & O'Brien, H. D. (2018). Mesowear study of ungulates from the early Pleistocene site of 'Ubeidiya (Israel) and the implications for early Homo dispersal from Africa. *Quaternary International*, *480*, 66–77. https://doi.org/10.1016/j.quaint.2017.03.052

Bermúdez De Castro, J. M., Martinón-Torres, M., Sier, M. J., & Martín-Francés, L. (2014). On the variability of the dmanisi mandibles. *PLoS ONE*, *9*(2). https://doi.org/10.1371/journal.pone.0088212

Blain, H. A., Agustí, J., Lordkipanidze, D., Rook, L., & Delfino, M. (2014). Paleoclimatic and paleoenvironmental context of the Early Pleistocene hominins from Dmanisi (Georgia, Lesser Caucasus) inferred from the herpetofaunal assemblage. *Quaternary Science Reviews*, *105*, 136–150. https://doi.org/10.1016/j.quascirev.2014.10.004

Blain, H. A., Fagoaga, A., Sánchez-Bandera, C., Ruiz-Sánchez, F. J., Sindaco, R., & Delfino, M. (2022). New paleoecological inferences based on the Early Pleistocene amphibian and reptile assemblage from Dmanisi (Georgia, Lesser Caucasus). *Journal of Human Evolution*, *162*. https://doi.org/10.1016/j.jhevol.2021.103117

Bräuer, G. (1988), Osteometrie. a. Kraniometrie. In: Knussmann R. (Ed.) Anthropologie. Handbuck der vergleichenden Biologie des Menschen. Bd. I: Wesen und methoden der Anthropologie. Stuttgart & New York: G. Fischer-Verlag

Chopra, S., Müller, N., Dhingra, D., Mani, I., Kaushik, T., Kumar, A., & Beaudry, R. (2022). A mathematical description of evaporative cooling potential for perishables storage in India. *Postharvest Biology and Technology*, *183*(July 2021). https://doi.org/10.1016/j.postharvbio.2021.111727

Dennell, R., & Roebroeks, W. (2005). An Asian perspective on early human dispersal from Africa. *Nature*, *438*(7071), 1099–1104. https://doi.org/10.1038/nature04259

Douka, K., Slon, V., Jacobs, Z., Ramsey, C. B., Shunkov, M. V., Derevianko, A. P., Mafessoni, F., Kozlikin, M. B., Li, B., Grün, R., Comeskey, D., Devièse, T., Brown, S., Viola, B., Kinsley, L., Buckley, M., Meyer, M., Roberts, R. G., Pääbo, S., … Higham, T. (2019). Age estimates for hominin fossils and the onset of the Upper Palaeolithic at Denisova Cave. *Nature*, *565*(7741), 640–644. https://doi.org/10.1038/s41586-018-0870-z

Efron, B., & Tibshirani, R. J. (1993). An introduction to the bootstrap. New York: Chapman and Hall

Ferring, R., Oms, O., Agustí, J., Berna, F., Nioradze, M., Shelia, T., Tappen, M., Vekua, A., Zhvania, D., & Lordkipanidze, D. (2011). Earliest human occupations at Dmanisi (Georgian Caucasus) dated

to 1.85-1.78 Ma. *Proceedings of the National Academy of Sciences of the United States of America*, *108*(26), 10432–10436. https://doi.org/10.1073/pnas.1106638108

Gabunia, L., Vekua, A., & Lordkipanidze, D. (2000). The environmental contexts of early human occupation of Georgia (Transcaucasia). *Journal of Human Evolution*, *38*(6), 785–802. https://doi.org/10.1006/jhev.1999.0383

Gabunia, L., Vekua, A., Lordkipanidze, D., Swisher, C. C., Ferring, R., Justus, A., Nioradze, M., Tvalchrelidze, M., Antón, S. C., Bosinski, G., Jöris, O., Lumley, M. A. D., Majsuradze, G., & Mouskhelishvili, A. (2000). Earliest Pleistocene hominid cranial remains from Dmanisi, Republic of Georgia: Taxonomy, geological setting, and age. *Science*, *288*(5468), 1019–1025. https://doi.org/10.1126/science.288.5468.1019

Galway-Witham, J., Cole, J., & Stringer, C. (2019). Aspects of human physical and behavioural evolution during the last 1 million years. *Journal of Quaternary Science*, *34*(6), 355–378. https://doi.org/10.1002/jqs.3137

Garvin, H. M., Elliott, M. C., Delezene, L. K., Hawks, J., Churchill, S. E., Berger, L. R., & Holliday, T. W. (2017). Body size, brain size, and sexual dimorphism in Homo naledi from the Dinaledi Chamber. *Journal of Human Evolution*, *111*, 119–138. https://doi.org/10.1016/j.jhevol.2017.06.010

Gibbons, A. (2013). Stunning Skull Gives a Fresh Portrait of Early Humans. *Science*, *342*(6156), 297–298. https://doi.org/10.1126/science.342.6156.297

Howells, W.W. (1973) Cranial Variation in Man. A Study by Multivariate Analysis of Patterns of Differences Among Recent Human Populations. Papers of the Peabody Museum of Archaeology and Ethnology, vol. 67. Cambridge, Mass.: Peabody Museum

Howells, W.W. (1989) Skull Shapes and the Map. Craniometric Analyses in the Dispersion of Modern Homo. Papers of the Peabody Museum of Archaeology and Ethnology, vol. 79. Cambridge, Mass.: Peabody Museum

Howells, W. W. (1996). Howells' craniometric data on the Internet. *American Journal of Physical Anthropology*, *101*(3), 441–442. https://doi.org/10.1002/ajpa.1331010302

Hurley, W. J. (2000). Resampling Calculations in a Spreadsheet. *Business*, *October*, 28–30.

Kottek, M., Grieser, J., Beck, C., Rudolf, B., & Rubel, F. (2006). World map of the Köppen-Geiger climate classification updated. *Meteorologische Zeitschrift*, *15*(3), 259–263. https://doi.org/10.1127/0941-2948/2006/0130

Lockwood, C. A., Richmond, B. G., Jungers, W. L., & Kimbel, W. H. (1996). Randomization procedures and sexual dimorphism in Australopithecus afarensis. *Journal of Human Evolution*, *31*(6), 537–548. https://doi.org/10.1006/jhev.1996.0078

Lordkipanidze, D., De Ponce León, M. S., Margvelashvili, A., Rak, Y., Rightmire, G. P., Vekua, A., & Zollikofer, C. P. E. (2013). A complete skull from Dmanisi, Georgia, and the evolutionary biology of early Homo. *Science*, *342*(6156), 326–331. https://doi.org/10.1126/science.1238484

Lordkipanidze, D., Jashashvili, T., Vekua, A., De León, M. S. P., Zollikofer, C. P. E., Rightmire, G. P., Pontzer, H., Ferring, R., Oms, O., Tappen, M., Bukhsianidze, M., Agusti, J., Kahlke, R., Kiladze, G., Martinez-Navarro, B., Mouskhelishvili, A., Nioradze, M., & Rook, L. (2007). Postcranial evidence

from early Homo from Dmanisi, Georgia. *Nature*, *449*(7160), 305–310. https://doi.org/10.1038/nature06134

Lordkipanidze, D., Vekua, A., Ferring, R., Rightmire, G. P., Zollikofer, C. P. E., De León, M. S. P., Agusti, J., Kiladze, G., Mouskhelishvili, A., Nioradze, M., & Tappen, M. (2006). A fourth hominin skull from Dmanisi, Georgia. *Anatomical Record - Part A Discoveries in Molecular, Cellular, and Evolutionary Biology*, *288*(11), 1146–1157. https://doi.org/10.1002/ar.a.20379

Lorenzo, C., Carretero, J. M., Arsuaga, J. L., Gracia, A., & Martínez, I. (1998). Intrapopulational body size variation and cranial capacity variation in middle pleistocene humans: The Sima de los Huesos sample (Sierra de Atapuerca, Spain). *American Journal of Physical Anthropology*, *106*(1), 19–33. https://doi.org/10.1002/(SICI)1096-8644(199805)106:1<19::AID-AJPA2>3.0.CO;2-8

Martinón-Torres, M., Bermúdez de Castro, J. M., Gómez-Robles, A., Margvelashvili, A., Prado, L., Lordkipanidze, D., & Vekua, A. (2008). Dental remains from Dmanisi (Republic of Georgia): Morphological analysis and comparative study. *Journal of Human Evolution*, *55*(2), 249–273. https://doi.org/10.1016/j.jhevol.2007.12.008

Mellars, P., & French, J. C. (2011). Tenfold population increase in Western Europe at the Neandertal-to-modern human transition. *Science*, *333*(6042), 623–627. https://doi.org/10.1126/science.1206930

Messager, E., Lordkipanidze, D., Delhon, C., & Ferring, C. R. (2010). Palaeoecological implications of the Lower Pleistocene phytolith record from the Dmanisi Site (Georgia). *Palaeogeography, Palaeoclimatology, Palaeoecology*, *288*(1–4), 1–13. https://doi.org/10.1016/j.palaeo.2010.01.020

Messager, E., Lordkipanidze, D., Ferring, C. R., & Deniaux, B. (2008). Fossil fruit identification by SEM investigations, a tool for palaeoenvironmental reconstruction of Dmanisi site, Georgia. *Journal of Archaeological Science*, *35*(10), 2715–2725. https://doi.org/10.1016/j.jas.2008.04.026

Plavcan, J. M., & Cope, D. A. (2001). Metric variation and species recognition in the fossil record. *Evolutionary Anthropology*, *10*(6), 204–222. https://doi.org/10.1002/evan.20001

Rightmire, G. P., Lordkipanidze, D., & Vekua, A. (2006). Anatomical descriptions, comparative studies and evolutionary significance of the hominin skulls from Dmanisi, Republic of Georgia. *Journal of Human Evolution*, *50*(2), 115–141. https://doi.org/10.1016/j.jhevol.2005.07.009

Rightmire, G. P., Margvelashvili, A., & Lordkipanidze, D. (2019). Variation among the Dmanisi hominins: Multiple taxa or one species? *American Journal of Physical Anthropology*, *168*(3), 481–495. https://doi.org/10.1002/ajpa.23759

Rightmire, G. P., Ponce de León, M. S., Lordkipanidze, D., Margvelashvili, A., & Zollikofer, C. P. E. (2017). Skull 5 from Dmanisi: Descriptive anatomy, comparative studies, and evolutionary significance. *Journal of Human Evolution*, *104*, 50–79. https://doi.org/10.1016/j.jhevol.2017.01.005

Saarinen, J., Oksanen, O., Žliobaitė, I., Fortelius, M., DeMiguel, D., Azanza, B., Bocherens, H., Luzón, C., Solano-García, J., Yravedra, J., Courtenay, L. A., Blain, H. A., Sánchez-Bandera, C., Serrano-Ramos, A., Rodriguez-Alba, J. J., Viranta, S., Barsky, D., Tallavaara, M., Oms, O., … Jiménez-Arenas, J. M. (2021). Pliocene to Middle Pleistocene climate history in the Guadix-Baza Basin, and the environmental conditions of early Homo dispersal in Europe. *Quaternary Science Reviews*, *268*. https://doi.org/10.1016/j.quascirev.2021.107132

Scardia, G., Neves, W. A., Tattersall, I., & Blumrich, L. (2021). What kind of hominin first left Africa? *Evolutionary Anthropology*, *30*(2), 122–127. https://doi.org/10.1002/evan.21863

Schuster, S. C., Miller, W., Ratan, A., Tomsho, L. P., Giardine, B., Kasson, L. R., Harris, R. S., Petersen, D. C., Zhao, F., Qi, J., Alkan, C., Kidd, J. M., Sun, Y., Drautz, D. I., Bouffard, P., Muzny, D. M., Reid, J. G., Nazareth, L. v., Wang, Q., … Hayes, V. M. (2010). Complete Khoisan and Bantu genomes from southern Africa. *Nature*, *463*(7283), 943–947. https://doi.org/10.1038/nature08795

Schwartz, J. H., Tattersall, I., & Chi, Z. (2014). Comment on "A Complete Skull from Dmanisi, Georgia, and the Evolutionary Biology of Early Homo ." *Science*, *344*(6182), 360–360. https://doi.org/10.1126/science.1250056

Scorrer, J., Faillace, K. E., Hildred, A., Nederbragt, A. J., Andersen, M. B., Millet, M.-A., Lamb, A. L., & Madgwick, R. (2021). *Diversity aboard a Tudor warship: investigating the origins of the Mary Rose crew using multi-isotope analysis*. https://doi.org/10.1098/rsos.202106

Shea, J. J. (2003). The Middle Paleolithic of the East Mediterranean Levant. *Journal of World Prehistory*, *17*(4), 313–394. https://doi.org/10.1023/B:JOWO.0000020194.01496.fe

Skinner, M. M., Gordon, A. D., & Collard, N. J. (2006). Mandibular size and shape variation in the hominins at Dmanisi, Republic of Georgia. *Journal of Human Evolution*, *51*(1), 36–49. https://doi.org/10.1016/j.jhevol.2006.01.006

Slon, V., Mafessoni, F., Vernot, B., de Filippo, C., Grote, S., Viola, B., Hajdinjak, M., Peyrégne, S., Nagel, S., Brown, S., Douka, K., Higham, T., Kozlikin, M. B., Shunkov, M. V., Derevianko, A. P., Kelso, J., Meyer, M., Prüfer, K., & Pääbo, S. (2018). The genome of the offspring of a Neanderthal mother and a Denisovan father. *Nature*, *561*(7721), 113–116. https://doi.org/10.1038/s41586-018-0455-x

Van Arsdale, A. P., & Lordkipanidze, D. (2012). A Quantitative Assessment of Mandibular Variation in the Dmanisi Hominins. PaleoAnthropology, 2012, 134–144. Retrieved from http://www.paleoanthro.org/journal/content/PA20120134.pdf

Vekua, A., Lordkipanidze, D., Rightmire, G. P., Agusti, J., Ferring, R., Maisuradze, G., Mouskhelishvili, A., Nioradze, M., De Leon, M. P., Tappen, M., Tvalchrelidze, M., & Zollikofer, C. (2002). A new skull of early Homo from Dmanisi, Georgia. *Science*, *297*(5578), 85–89. https://doi.org/10.1126/science.1072953

White T. D. Black M. T. & Folkens P. A. (2012). Human osteology (Third). Elsevier/Academic Press

APPENDIX BOOTSTRAP USING EXCEL 2019

The purpose of this Appendix is to provide a guide to using the Table function of Excel 2019 to perform bootstrap analysis.

In Figure 30 the data from Figure 1 of Hurley, 2000 is reproduced. The numbers in "Sample Values" represent the result of an experiment in which seven randomly selected mice were subjected to a novel treatment to prolong life after surgery. A further nine mice made up the control group. The data shows the survival time in days after surgery of the 16 mice. Did the treatment successfully prolong survival after surgery?

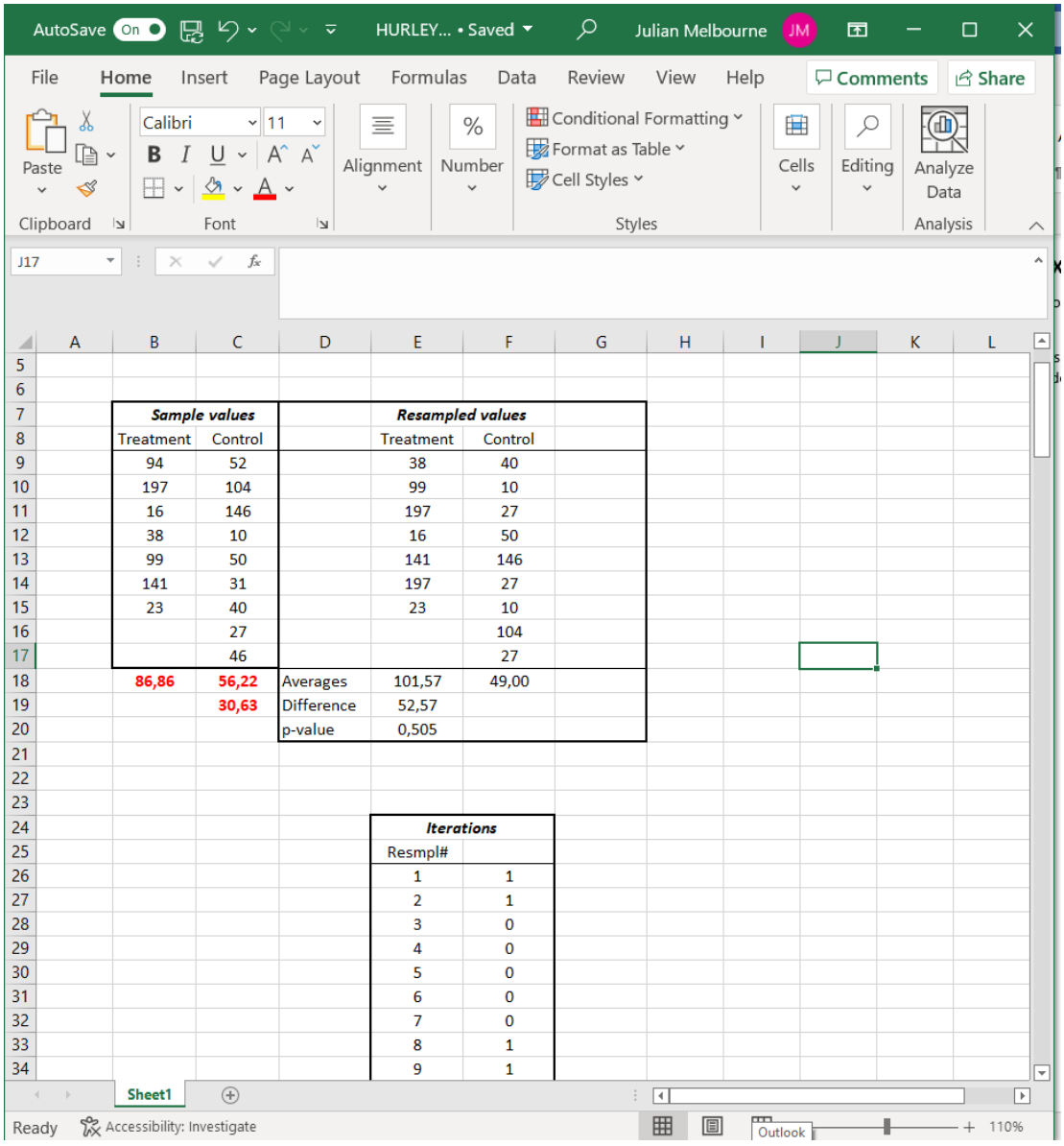

	Sample values			Resampled values	
	Treatment	Control		Treatment	Control
	94	52		38	40
	197	104		99	10
	16	146		197	27
	38	10		16	50
	99	50		141	146
	141	31		197	27
	23	40		23	10
		27			104
		46			27
	86,86	56,22	Averages	101,57	49,00
		30,63	Difference	52,57	
			p-value	0,505	

Iterations	
Resmpl#	
1	1
2	1
3	0
4	0
5	0
6	0
7	0
8	1
9	1

Figure 30. *Data reproduced from Figure 1 of Hurley, 2000, using the same Excel column letters and row numbers. The numbers in red, the average of the treatment sample values and control sample values, and their difference, have been added to the table for clarity.*

The new treatment appears to prolong life as the treated group survived an average of 86,86 days versus 56,22 for the control group, an improvement of 30,63 days. However, there is much variability in the data and the difference could be the result of chance. Instead of repeating the

experiment with the related costs and delays, sampling with replacement – bootstrapping – allows us to randomly select results from the experiment N times and then calculate a probability that the resampled results have a difference in excess of 30,63 days under the null hypothesis that the treatments are the same.

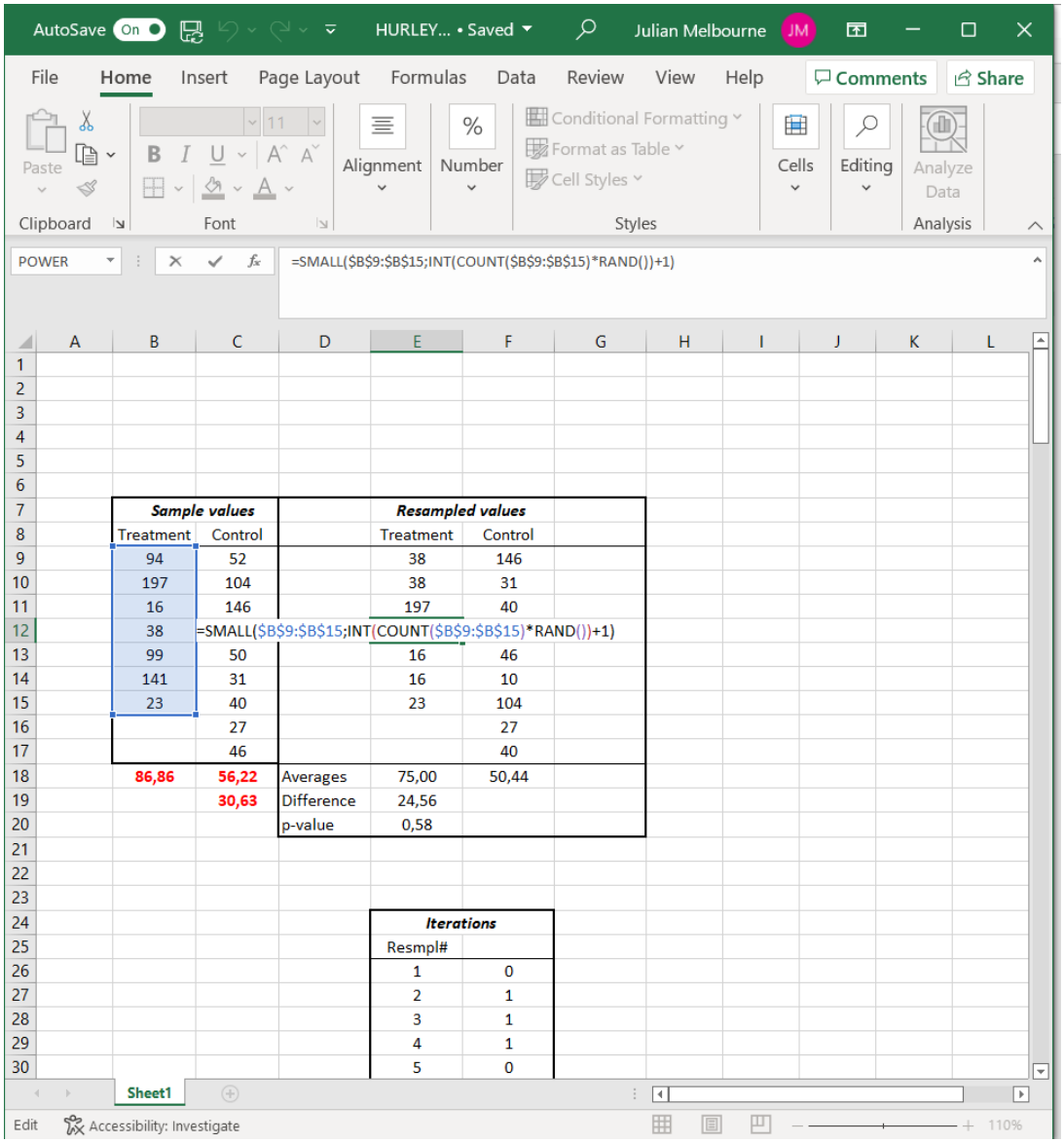

Figure 31. *Detail of the functions used in cell E12 to perform the resampling of the treated mice group.*

Figure 31 shows the detail of the formula that is used to select with replacement the samples from the treated mice group. The same formula is repeated in all cells E9 to E15. A similar formula for resampling the control group is used in cells F9 to F17. It refers to the control group sample values in C9 to C17:

=SMALL($C$9:$C$17;INT(COUNT($C$9:C$17)*RAND())+1)

It should be noted that the Hurley, 2000 paper was published by a Canadian institution and therefore Excel is shown using the North American convention of a comma to separate the variables in a formula. The convention in Europe, as seen above, is to use a semicolon.

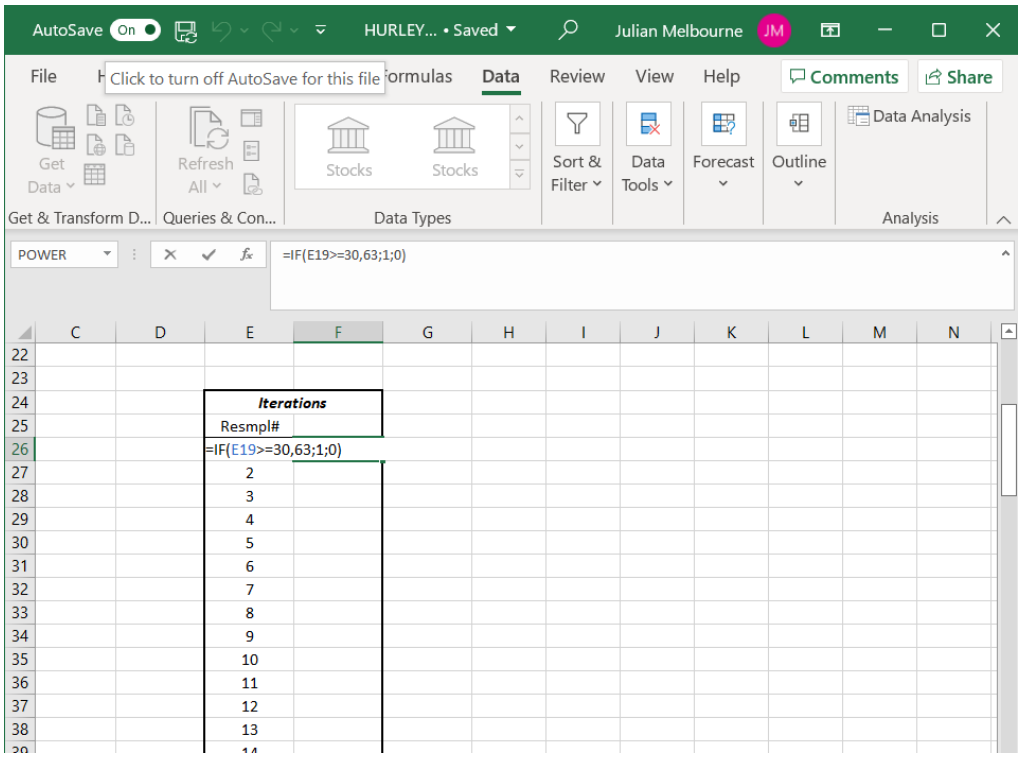

Figure 32. *Detail of the function in cell F26*

To carry out the resampling, each time recording whether the difference exceeds 30,63, we use the Excel Data Table function. We list from 1 to 200 in column E the iterations we are going to perform – in this case 200 as performed by Hurley, 2000. Cell F26 has the key formula:

=IF(E19>=30,63;1;0)

which checks the resampled difference in means. If it is equal to or greater than 30,63 it returns a 1, it is less then it returns a 0.

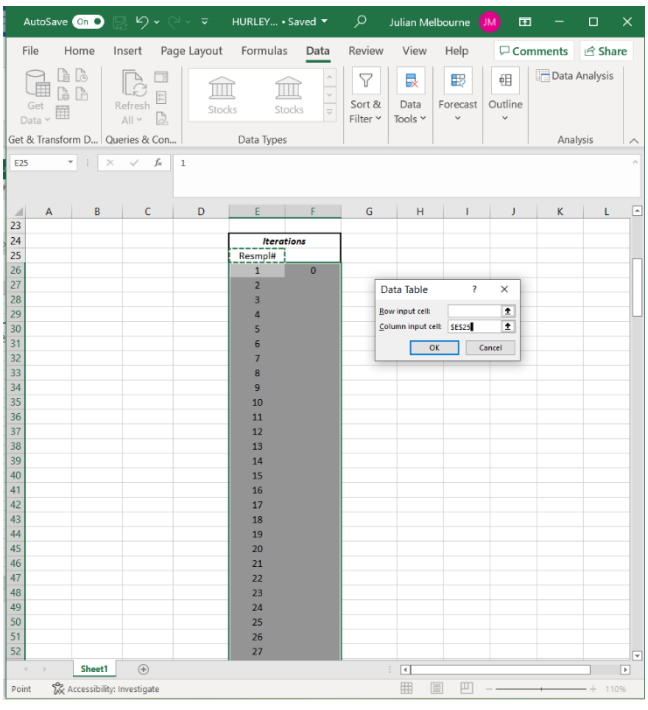

The next step is to highlight the 200 iteration rows as shown in Figure 33 where we have selected the two columns E and F from row 26 to row 225, ie the area E26 to F225. Then we need to find the Data Table function by clicking the menus:

Data / What-If Analysis / Data Table

Note the important dialogue box that appears in Figure 33. A column input cell needs to be chosen, and the best cell for this purpose is the top cell of the column of iterations – in this case E25. This was the recommendation of Hurley, 2000 with which this author concurs.

Figure 33. *Creation of Data Table in Excel*

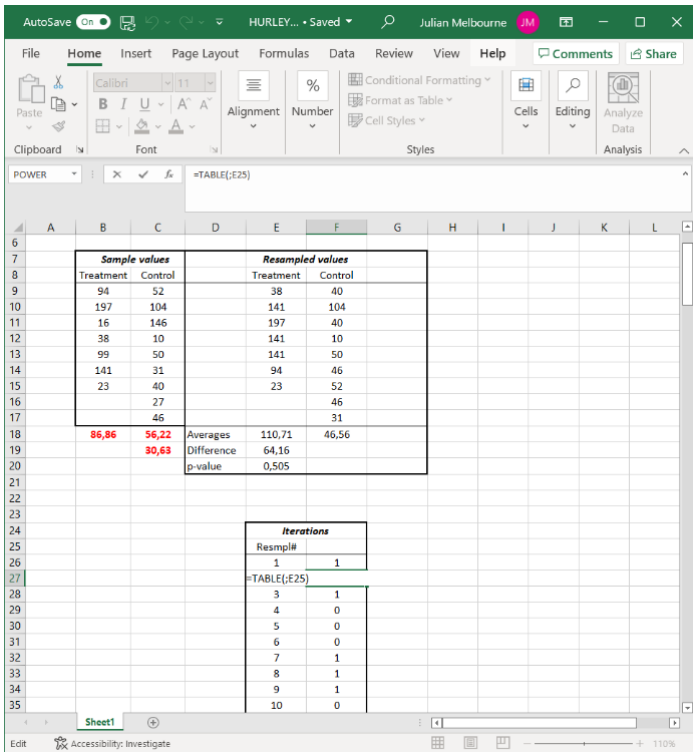

Figure 34 shows the finished file with an example of the content of the first cell completed by the Data Table function in Excel. All the cells from F27 to F225 will have the same content.

Cell E20 in Figure 34 shows the average of cells F26 to F225. Pressing the F9 button or clicking on Formulas / Calculate Now will cause the resampling to be recalculated and a slightly different value will emerge.

The p-value returned in Figure 34 is 0,505, and in Figure 31 it is 0,58. The result in Hurley, 2000 was 0,475. The conclusion is that there is not sufficient evidence to confirm that the difference in treatments is 30,63 days or more.

Figure 34. *Completed data table with detail of the content of cell F26*

It should be noted that the above example is based on 200 resampling iterations and gives a p-value in the approximate range of 0,475 to 0,58. Performing the same exercise with 5000 iterations narrows the result to approximately 0,484 to 0,512.